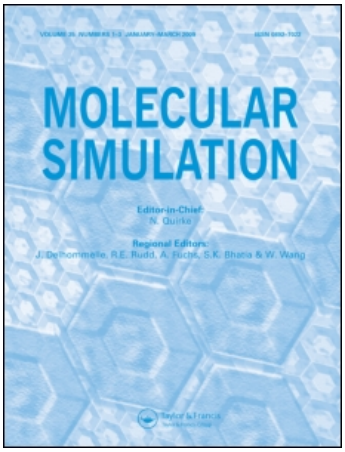

Molecular Simulation
Publication details, including instructions for authors and subscription information:
http://www.informaworld.com/smpp/title~content=t713644482

Four Important Factors in the *ab initio* Determination of Accurate Inter-Ionic Potentials

N. C. Pyper[a]
[a] University Chemical Laboratory, Cambridge, U.K.

To cite this Article Pyper, N. C.(1990) 'Four Important Factors in the *ab initio* Determination of Accurate Inter-Ionic Potentials', Molecular Simulation, 5: 1, 23 — 81
To link to this Article: DOI: 10.1080/08927029008022409
URL: http://dx.doi.org/10.1080/08927029008022409

Molecular Simulation, 1990, Vol. 5, pp. 23–81
Reprints available directly from the publisher
Photocopying permitted by license only

FOUR IMPORTANT FACTORS IN THE *AB INITIO* DETERMINATION OF ACCURATE INTER-IONIC POTENTIALS

N.C. PYPER

University Chemical Laboratory, Lensfield Road, Cambridge, CB2 1EW, U.K.

(*Received September 1989, accepted September 1989*)

The accurate *ab initio* determination of inter-ionic potentials requires the consideration of four important factors. These are relativistic effects for ions of high atomic number, the environmentally induced modifications of ion wavefunctions, the damping of reliably calculated inter-ionic dispersive attractions and the avoidance of density functional descriptions of the uncorrelated potentials.

The relativistic modifications of the behaviour of valence electrons in elements heavier than those of the third series of transition elements are too large to be treated by first order perturbation theory. The relativistic integrals programme (RIP), which works directly with the Dirac equation and four component wavefunctions for the individual electrons, is used to compute fully relativistic inter-ionic potentials.

The mechanisms through which ion wavefunctions are modified by their environment in the crystal are discussed. A simple yet physically realistic model for computing such wavefunctions is presented. The contractions of anion wave functions caused by their environment in the crystal are shown to be sufficiently significant that the use of free ion wavefunctions is inadequate for accurate work. The crystalline environment leaves unaffected the wavefunctions and polarizabilities of cations having s^2 or p^6 outermost electronic configurations.

The inter-ionic dispersive (van der Waals) attractions are shown to contribute significantly to the crystal cohesion. The overlap of the ion wavefunctions damps these attractions sufficiently that predictions derived neglecting this damping are unreliable. A trustworthy method for deriving values of dipole–dipole dispersion coefficients for ions in crystals is presented.

Density functional predictions of inter-ionic potentials are tested against the RIP programme which yields results that are exact once the ion wavefunctions have been specified. Density functional theory must be judged to fail for many cation–cation and anion–anion interactions because its predictions bear little relation to those derived from RIP calculations. Although density functional theory gives a fair account of the cohesion of many crystals, the use of RIP rather than density functional potentials significantly improves the predictions. Density functional theory fails for AgF.

KEY WORDS: *Ab initio*, inter-ionic potentials, relativistic effects, relativistic integrals programme, dispersion energy, density functional theory.

0. MOTIVATION AND THEORETICAL BACKGROUND

0.1 Introduction

In the proceedings of a conference whose title is 'The Practical computation of inter-ionic potentials', it is hardly necessary to start with a long review justifying the need to compute such potentials. This has not only been done previously [1–4] but also such justifications can be found in the introduction to a review [5] of the *ab initio* computation of potentials that is in the last stages of completion. The object of this talk is not to present a thorough review of the computation of potentials because this can be found in [5] but rather to highlight four important features that need to be

considered when undertaking such calculations. The first of these is the role of relativity in modifying the behaviour of the electrons in ions of high atomic number thereby affecting the inter-ionic potentials. The second is the role that the environment of an ion in an ionic crystal plays in modifying the wavefunction of that ion when compared with that of the isolated ion. Any such modifications will naturally be reflected in the inter-ionic potentials. The third is the importance of introducing a reliably calculated dispersion energy which includes its damping [6,7] that arises when the overlap of the wavefunctions of the interacting ions is not negligible. The fourth is desirability of avoiding the use of density functional theory [8,9] to calculate the uncorrelated short range potentials. These four features are discussed in the sections 1 to 4 respectively. The remainder of this preliminary section (zero) merely presents the definitions and basic theory to be used.

The four features forming the subject matter of this talk can be illustrated without considering systems more complicated than perfect cubic crystals of stoichiometry CA_m containing only one type of cation, denoted C, and one kind of anion (A) both of which have spherically symmetric charge distributions. Furthermore it will be assumed that the crystal is fully ionic so that each ion carries a charge that is an integral multiple of the charge on an electron and that the anion in the free gaseous state is stable with respect to the loss of an electron. The last requirement excludes the doubly charged oxide and chalcogenide ions because in the isolated state each of these is unstable with respect to the singly charged ion and a free electron [10].

Currently there seem to be two fundamentally different approaches for investigating *ab initio* the properties of ionic crystals. In the first of these, it is assumed that the total electronic wavefunction of the crystal can be written as an anti-symmetrized product of the wavefunctions of the individual ions thereby enabling the cohesive energy to be expressed as the sum of pairwise additive inter-ionic potentials augmented by higher order multi-body terms [4,11]. In the second, Hartree-Fock theory with periodic boundary conditions is used to compute an electronic wavefunction for an entire unit cell [12–14]. This second approach is more general than the first in that it is not assumed that the crystal is ionic so that it can be applied even to essentially covalent materials such as diamond [15,16] and boron nitride [17,18]. However an inevitable consequence of the generality of this method is that one loses the ability to decompose the cohesive energy into a sum of potentials augmented by smaller multi-body corrections that is such a valuable feature of the first approach. Indeed if the degree of covalency is significant, it would clearly be impossible to extract from such computations the inter-ionic potentials that are the subject of this article. It is beyond the scope of this talk to debate the relative merits of the two approaches. In this article, the first approach will be used. This choice was made for two reasons. Firstly it is the quantum mechanical formulation of the fully ionic model for a crystal and, secondly, only in this approach is it currently possible to perform the fully relativistic calculations based on the Dirac equation which are necessary when dealing with systems containing ions of high atomic numbers. Even if the second approach were to be used, it would still be necessary to consider the four factors with which this talk is concerned.

0.2 Physical Model For The Crystal Formation

The basic physical model for the CA_m crystal is that it is composed of cations and anions whose electronic charge distributions are optimal for the crystal geometry

considered subject to the proviso that each ion is spherically symmetric and contains a fixed integral number of electrons. For a uniform expansion or contraction of a cubic crystal from the equilibrium positions of the nuclei of the ions, the geometry is completely defined by the closest cation–anion separation denoted R. The value of R at the equilibrium positions of the nuclei is denoted R_e. For any given value of R the crystal can be regarded as having been assembled from free isolated ions in two stages.

In the first stage, each of the isolated ions is modified to a non-stationary state which is optimal for the crystalline environment in the sense that the total energy of the crystal is minimised when, in the second stage, the modified ions are assembled to form the crystal. At the end of the first stage, all the ions from which the crystal is assembled are still isolated from each other and thus still non-interacting. For each ion X, where X is either a cation C or an anion A, the energy ($E_X(R)$) of the ion in the isolated non-stationary state is less negative than the energy (E_X) of an isolated ion X in its electronic ground state. The positive energy needed to convert the isolated ion X in its electronic ground state to the state optimal for the crystal having closest cation–anion separation R will be called the rearrangement energy of ion X and denoted $E^X_{Re}(R)$. This is given by

$$E^X_{Re}(R) = E_X(R) - E_X \tag{1}$$

The energy (E_X) of the free ion X is not only the eigenvalue resulting when the Hamiltonian of the free ion acts on the ground state wavefunction but is also the expectation value of this wavefunction calculated using the same free ion Hamiltonian. The wavefunction for the ion in the non-stationary state optimal for the crystal is not an eigenfunction of the free ion Hamiltonian, the state being non-stationary, so that the meaning of the energy $E_X(R)$ is that it is the expectation value of the free ion Hamiltonian calculated using the wavefunction of the ion X in its state optimal for the crystal. In physical terms, $E_X(R)$ is the energy of an isolated X ion having, not the ground state wavefunction, but the non-stationary wavefunction optimal for the crystalline environment arising in the second stage. The total rearrangement energy, denoted $E^T_{Re}(R)$, per formula unit of a crystal CA_m is therefore given by

$$E^T_{Re}(R) = E^C_{Re}(R) + mE^A_{Re}(R) \tag{2}$$

It is not useful to think of the electronic structures of the ions in their states optimal for the crystal as having different electronic configurations from those of the free ions because the ion wavefunctions optimal for the crystal usually only differ from their free ion counterparts by an expansion or contraction in space of the electron density distribution. The mathematical formulation of the calculation of the crystal cohesive energy presented in the next subsection shows that this is indeed the case. A schematic energy level diagram showing how the ion rearrangement energies act to reduce the total cohesive energy of the crystal is presented in Figure 1.

In the second of the two stages in which the crystal is regarded as being assembled, the isolated gaseous ions in their non-stationary states are assembled to form the crystal having geometry specified by the closest cation–anion separation R. Per formula unit CA_m the total energy, denoted $E_{CA_m}(R)$, of this crystal, is equal to the sum of the purely electronic part plus that arising from all the inter-nuclear repulsions. Hence the binding energy ($V_L(R)$) of this crystal relative to the sum of the energies of one cation plus m anions each in the isolated but non-stationary states generated by the first stage is given by

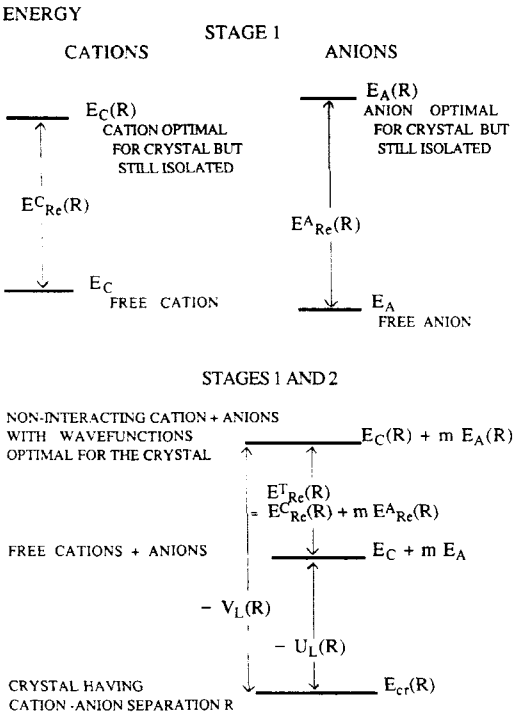

Figure 1 Energy Level Diagram for the formation of the crystal from its constitutent ions.

$$V_L(R) = E_{CA_m}(R) - E_C(R) - mE_A(R) \tag{3}$$

The quantity $V_L(R)$ is negative if energy is released in the second stage as is the case except for values of R very much smaller than the equilibrium value R_e. For all but very small R, the electrostatic interactions between the ions are the largest contributors to $V_L(R)$ although shorter range repulsive forces originating from the overlap of the ion wavefunctions are far from negligible.

The binding energy ($U_L(R)$) of the crystal measured relative to the sum of the energies of one cation and m anions all in their electronic ground states is the sum of the energy changes occurring in the first and second stages and is therefore given by

$$U_L(R) = E^T_{Re}(R) + V_L(R) \tag{4}$$

The quantity $U_L(R)$ is negative if the crystal having closest cation-anion separation R is bound relative to the free ions in their electronic ground states. Figure 1 illustrates how for a bound crystal ($U_L(R) < 0$), the energy ($-V_L(R)$) released on forming the crystal from the ions in their non-stationary states is partially counteracted by the rearrangement energy ($E^T_{Re}(R)$) to yield a binding energy smaller in magnitude than $V_L(R)$. As discussed in section 0.4, the physical model just described for the formation of the crystal does not implicitly neglect the effects of electron correlation.

0.3 *Mathematical Formulation Excluding Electron Correlation*

The precise mathematical meaning of the assumption that the crystal is fully ionic will be taken to be that the wavefunction for all the electrons in the crystal is able to be factorized into an anti-symmetrized product of wavefunctions for the individual ions. If electron correlation, discussed in the next subsection, is neglected, each of the individual ion wavefunctions reduces to a single anti-symmetrized product of one-electron orbitals. Although these orbitals could be taken to be those of the free isolated ions, the crystalline environment will cause those orbitals best describing the solid having geometry defined by R to differ from those of the free ions. Whatever the exact form of the individual one-electron orbitals, the total energy $E_{cr}(R)$ of the crystal containing N_{ion} ions can be expressed exactly as a sum of 1-body, 2-body up to N_{ion} -body terms [11]. Thus

$$E_{cr}(R) = \sum_{a=1}^{N_{\text{ion}}} E_a(r) + \sum_{a=1}^{N_{\text{ion}}-1} \sum_{b=a+1}^{N_{\text{ion}}} V_{ab}^0(x_{ab}R) + \sum_{a=1}^{N_{\text{ion}}} \sum_{b\neq a} \sum_{c\neq b} + \ldots \qquad (5)$$

Here the label a distinguishes between the different ions rather than between the different types of ion. Thus, for example, an NaCl crystal contains many different Na^+ ions distinguished by different labels a with the label C introduced in the last subsection denoting the type of ion, namely a cation. For a crystal containing one mole of the formula unit CA_m, $E_{cr}(R)$ becomes identical to the energy $E_{CA_m}(R)$ introduced in the last subsection provided that the latter energy is expressed as an energy per mole.

For a crystal containing one mole of the formula unit CA_m, the first summation in (5) reduces to

$$\sum_{a=1}^{N_{\text{ion}}} E_a(R) = E_C(R) + m\,E_A(R) \qquad (6)$$

where the energies $E_C(R)$ and $E_A(R)$ introduced in the last subsection are expressed as energies per mole. The expression (6) describes a 1-body contribution to the energy because, each term containing only the wavefunction of a single ion, does not involve any interactions between the ions given that these are in the appropriate non-stationary states. This terminology differs from that of Muhlhausen and Gordon [19] who designated any modification of the ion wavefunctions from those of the free ion ground states to be a many-body effect. These authors would therefore say that (6) contains many-body contributions unless this is evaluated using the ground state wavefunctions of the free ions. However, although it is true that such wavefunction modifications are caused by those portions of the potential acting on an electron on one ion which originate from a large number of neighbouring ions, the expression $E_a(R)$, containing only the wavefunction of a single ion, is not a many-body energy in the sense of involving either the wavefunctions of several ions or Hamiltonian terms originating from other ions in the crystal. Thus the Hamiltonian, whose expectation value is the energy $E_a(R)$, contains only those terms entering the Hamiltonian of the free ion a. The terminology of [19] will not therefore be used even though it is a valid alternative definition of the term 'many-body'.

The double and higher order summations in (5) constitute the contribution to $E_{cr}(R)$ which arises from the interactions between the ions having the non-stationary wavefunctions optimal for the crystal with geometry defined by R. The quantity x_{ab}

is a purely geometrical constant which relates the distance $(x_{ab}R)$ between the two ions a and b to the closest cation–anion separation R. For one mole of formula unit CA_m the sum of the double and higher order summations in (5) therefore reduces to the quantity $V_L(R)$ provided that this is expressed as an energy per mole. Denoting this quantity $V_L^0(R)$, the superscript 0 denoting that $V_L(R)$ is evaluated with the neglect of electron correlation, one has [11]

$$V_L^0(R) = \sum_{a=1}^{N_{\text{ion}}-1} \sum_{b=a+1}^{N_{\text{ion}}} V_{ab}^0(x_{ab}R) + \sum\sum\sum + \ldots \tag{7}$$

This demonstration that the crystal energy is the sum of the two contributions (6) and (7) provides the mathematical justification for the physical model of the crystal formation which was described in the last subsection.

The quantity $V_{ab}^0(x_{ab}R)$ is just the energy of interaction of the pair of ions a and b separated by a distance $x_{ab}R$ and having the non-stationary wavefunctions optimal for the crystal geometry defined by R. Since this interaction energy depends solely on the pair of ions a and b and their separation $x_{ab}R$ and moreover is entirely independent of the remainder of the crystal after specifying the orbitals used to construct the ion wavefunctions, $V_{ab}^0(x_{ab}R)$ is a 2-body energy. In atomic units (a.u.) the total charge, denoted q_a, carried by ion a is given by the difference $Z_a - N_a$ where Z_a and N_a are respectively the nuclear charge and number of electrons on ion a. It is convenient to decompose $V_{ab}^0(x_{ab}R)$ into the point coulombic value $q_a q_b/(x_{ab}R)$ a.u. it would have if the overlap between the spherical ion wavefunctions was negligible plus a remainder $V_{sab}^0(x_{ab}R)$ which arises entirely from ion wavefunction overlap. The overlap has two consequences. Firstly it causes the total kinetic energy of the electrons in the interacting pair to be greater than that in the non-interacting pair of ions each in its non-stationary state optimal for the crystal. Secondly overlap causes the total electrostatic interaction between the two ions to differ from the point coulombic value $q_a q_b/(x_{ab}R)$. This total electrostatic interaction includes the contribution that originates from the exchange of electrons between the ions. Hence one defines

$$V_{ab}^0(x_{ab}R) = V_{sab}^0(x_{ab}R) + q_a q_b/(x_{ab}R) \tag{8}$$

The separation (8) is useful because the point coulomb terms which are thus seen to enter (5) and (7) decrease only very slowly with increasing $x_{ab}R$ and constitute a Madelung sum. The remaining terms $V_{sab}^0(x_{ab}R)$ decrease rapidly with increasing $x_{ab}R$ and are therefore designated short-range potentials as indicated by the subscript s. It is therefore only necessary to consider a few near neighbour short-range terms whilst the Madelung sum is standard. If only the nearest cation–anion, cation–cation and anion–anion short range interactions are retained and the triple and higher order summations in (7) are neglected, it immediately follows that

$$V_L^0(R) = -M/R + n_{CA}V_{sCA}^0(R) + (1/2)\{n_{CC}V_{sCC}^0(x_{CC}R) + m\,n_{AA}V_{sAA}^0(x_{AA}R)\} \tag{9}$$

Here M is the Madelung constant and n_{XY} is the number of nearest neighbour ions of type Y around each ion of type X whilst the labels CA, CC and AA denote one closest cation–anion, one closest cation–cation and one closest anion–anion pair respectively. The summations in (7) that are neglected in the derivation of (9) are 3-body and higher order multi-body contributions to the energy. Our current knowledge of these is reviewed elsewhere [5].

In the approximation that $V_L(R)$ is given by (9), the total crystal energy (5) per mole of formula unit CA_m is given by adding to $V_L^0(R)$ the 1-body energy (6), so that

$$E_{cr}(R) = E_{CA_m}(R) = V_L^0(R) + E_C(R) + m\,E_A(R) \tag{10}$$

The binding energy of the crystal measured relative to the energies of the free ions in their ground states is derived by subtracting from (10) the sum $E_C + mE_A$ of these ground state energies. Hence in the approximation in which electron correlation is neglected this binding energy, denoted $U_L^0(R)$, is seen after invoking the definitions (1) and (2) to be given by

$$U_L^0(R) = V_L^0(R) + E_{Re}^T(R) \tag{11}$$

with $V_L^0(R)$ taking the explicit form (9). The expression (11) differs from the result (4) presented in the last section on the basis of physical arguments solely by using the approximation in which electron correlation is neglected.

0.4 Electron Correlation Effects

0.4(i) Overview

For ionic crystals, electron correlation can be defined as those tendencies of electrons to avoid each other that are neglected when the crystal wavefunction is written as a single anti-symmetrized product of ion wavefunctions each of which is further approximated as a single anti-symmetrized product of orthonormal orbitals. One can distinguish two different types of correlation, namely intra-ionic electron correlation and inter-ionic electron correlation. The intra-ionic electron correlation is the correlation between electrons all of which belong to the same ion whilst the inter-ionic electron correlation is that involving electrons some of which are on different ions.

0.4(ii) Intra-ionic electron correlation

Intra-ionic electron correlation can be accounted for by removing the approximation of writing each of the individual ion wavefunctions as a single anti-symmetrized product. Such correlation could, in principle, contribute to the cohesive energy in two different ways. The first is by modifying the rearrangement energies $E_{Re}^X(R)$ and the second is by changing the energy $(-V_L(R))$ which is released when the crystal having closest cation–anion separation R is assembled from the ions in their isolated but non-stationary states.

For cations, the rearrangement energies $E_{Re}^C(R)$ are found to be extremely small [4], being less than 0.02 kJ mole^{-1} for Li^+, Na^+ and Mg^{++} when computed neglecting electron correlation and using the best of the models for the crystalline environment described in section 2. Furthermore, for Ag^+ and Pb^{++} the largest rearrangement energies thus computed [4] were 2.1 kJ mole^{-1} for AgF at $R = 3.5$ a.u. and 3.3 kJ mole^{-1} for PbF_2 at $R = 4.0$ a.u.. The rearrangement energies computed [4] for the F^- and Cl^- ions are significantly larger than those of the cations, lying in the range 41 kJ mole^{-1} to 133 kJ mole^{-1} for the smallest values of R considered (see Appendix 5 of [4]). However for values of R in the vicinity of the equilibrium value (R_e), these halide ion rearrangement energies are much smaller lying in the range 9 kJ mole^{-1} to 15 kJ mole^{-1} although they are still significantly larger than the cation rearrangement energies [4]. However the rearrangement energies of both cations and halide ions are sufficiently small that the contributions from electron correlation are probably of only marginal significance since these can be expected to amount to no more than some

10%–15% of the rearrangement energies. In view of this prediction, the correlation contributions to the rearrangement energies of these ions will henceforth be neglected because no quantitive studies of these correlation energies have so far been reported. For the oxide ion, the correlation contribution to the rearrangement energy cannot be neglected as discussed elsewhere [4,5,19].

The second way in which intra-ionic electron correlation can, in principle, influence the properties of an ionic crystal is by modifying the energy $V_L(R)$. This correlation will affect the size of the ions even if this effect is small, thereby providing at least one mechanism for this modification. The influence of such correlation on $V_L(R)$ has not yet been investigated quantatively because, for ionic crystals, *ab-initio* computations are at a sufficiently early stage of development that, even with the intra-ionic correlation neglected, it has only recently become possible to carry out such calculations reliably. The *ab-initio* calculations neglecting the intra-ionic correlation have achieved a considerable degree of success. The possible modifications of $V_L(R)$ by intra-ionic electron correlation will be neglected because such effects can be expected to alter the predicted crystal properties only slightly.

0.4(iii) Inter-ionic electron correlation

The inter-ionic electron correlation arises from the correlation of the motions of groups of electrons not all of which belong to the same ion. Discussion of such correlation is best started by considering just the interaction between a single pair of ions a and b embedded in the crystal. In the absence of inter-ionic electron correlation, the wavefunction for this pair of ions is given by a single anti-symmetrized product of the wavefunctions of the individual ions. The energy originating from inter-ionic electron correlation is obtained by using perturbation theory to derive a more accurate wavefunction for this pair of ions using the method presented in [20] which is outlined in section 3. This procedure shows that the interaction energy $V_{ab}(x_{ab}R)$ between the pairs of ions a and b separated by the distance $x_{ab}R$ is given by

$$V_{ab}(x_{ab}R) = V^0_{ab}(x_{ab}R) + V^{corr}_{sab}(x_{ab}R) + V^{disp}_{ab}(x_{ab}R) \qquad (12)$$

Here $V^0_{ab}(x_{ab}R)$ is the interaction energy (8) that is calculated neglecting the inter-ionic electron correlation whilst the two remaining terms arise from this correlation. The quantity $V^{corr}_{sab}(x_{ab}R)$ is the sum of three terms which were described as a pair of coupled exchange polarization terms and an exchange-exchange interaction [20]. Each of these three terms arises from the exchange of electrons between the ions and is therefore only non-zero if the overlaps between the wavefunctions of the pairs of ions do not vanish. Since these overlaps decay approximately exponentially with increasing $x_{ab}R$, the energy $V^{corr}_{sab}(x_{ab}R)$ decays exponentially also and vanishes for values of $x_{ab}R$ that are sufficiently large that the overlap of the ion wavefunctions has become negligible. Hence $V^{corr}_{sab}(x_{ab}R)$ is a short range term as designated by the subscript s. Since this is the only property of $V^{corr}_{sab}(x_{ab}R)$ required here, it is not necessary to present it in detail. In contrast to the short range interaction $V^{corr}_{sab}(x_{ab}R)$, the last energy in (12) $V^{disp}_{ab}(x_{ab}R)$ is of long range in that it does not vanish when the overlaps between the wavefunctions of the ions become negligible. This term, which is still valid even when these overlaps are non-zero, constitutes the dispersive or Van der Waals (London) attraction between the two ions. This term is discussed more fully in section 3.

After neglecting 3-body and higher order multi-body terms, the total inter-ionic electron correlation energy of a crystal is given by summing the last two terms of (12)

over all pairs of ions in the crystal. Since it is the non-vanishing of the overlap of the ion wavefunctions which causes the short range correlation terms $V_{sab}^{corr}(x_{ab}R)$ to be non-zero, these will be negligible for CA_m crystals except within the closest cation–anion, anion–anion and cation–cation pairs. It is therefore useful to regard these terms as corrections to the uncorrelated short range potentials $V_{sXY}^{0}(x_{XY}R)$ and to define total short range potentials by

$$V_{sXY}^{T}(x_{XY}R) = V_{sXY}^{0}(x_{XY}R) + V_{sXY}^{corr}(x_{XY}R) \tag{13}$$

The binding energy $U_L(R)$ of the crystal relative to that of its constituent ions in their isolated ground electronic states is given by adding the contribution from inter-ionic electron correlation to the expression (11) for $U_L^0(R)$. The result is

$$U_L(R) = -M/R + n_{CA}\, V_{sCA}^{T}(R) + (1/2)\{n_{CC}\, V_{sCC}^{T}(x_{CC}R) + m\, n_{AA}\, V_{sAA}^{T}(x_{AA}\, R)\} + E_{Re}^{C}(R) + m\, E_{Re}^{A}(R) + U_{disp}(R) \tag{14}$$

where $U_{disp}(R)$ is the total contribution from dispersion that results from summing the terms $V_{ab}^{disp}(x_{ab}R)$ over all pairs of ions. The result (14) differs from that $U_L^0(R)$ derived neglecting inter-ionic electron correlation solely in the use of short-range interactions containing a correlation correction and in the additional appearance of the dispersion energy.

0.5 *Techniques Of Calculation*

If electron correlation is neglected, the predicted properties of the crystal are determined by the function $U_L^0(R)$ (11) which is the sum of the rearrangement energy (2) and the binding energy $V_L^0(R)$ (9) measured relative to that of the non-interacting ions in the non-stationary states optimal for the crystalline environment. This form for $V_L^0(R)$ is used for all the calculations described here unless stated explicitly to the contrary.

Calculation through (1) of the rearrangement energy of each ion X requires knowledge of both the energy (E_X) of the free ion X in its ground electronic state and that ($E_X(R)$) of the isolated ion in its non-stationary state. The energy (E_X) can be obtained directly from a standard run of the Oxford atomic Dirac-Fock programme [21] which is used to compute the relativistic wavefunctions for the individual ions. The wavefunctions for the ions in the non-stationary states can be generated by using a version of this programme modified by incorporating a potential describing the influence of the crystalline environment on an electron belonging to ion X. Models for representing this potential are presented in section 2. The energy $E_X(R)$ can then be computed as the expectation value over the free ion Hamiltonian by using the atomic energy analysis programme. This programme is one of those belonging to the suite of programmes used to enhance the usefulness of the Oxford Dirac-Fock programme.

The binding energy $V_L^0(R)$ measured relative to the sum of the energies $E_X(R)$ is readily calculated from (9) provided that each of the short range energies $V_{sXY}^{0}(x_{XY}R)$ has been derived from (8) by subtracting the point coulomb term $q_Xq_Y/(x_{XY}R)$ from the interaction energy $V_{XY}^{0}(x_{XY}R)$ of the pair of ions X and Y. These interaction energies were computed using the Relativistic Integrals Programme (RIP) [22–24] which yields a result that is exact once the wavefunctions for the individual ions have been computed. This programme, described in detail in section 1.4, takes full account of relativistic effects. These are important for ions of high atomic number.

The short range correlation potential $V_{sXY}^{corr}(x_{XY}R)$ is a sum of the three terms, mentioned above, for which definitive quantum mechanical expressions have been presented [20]. Although each of the three terms could, in principle, be evaluated numerically from these expressions, it can be expected that such computations would, in practice, be highly cumbersome. Indeed the present author is not aware that such computations have been carried out for any pair of atomic species. Such calculations of $V_{sXY}^{corr}(x_{XY}R)$ have certainly not yet been carried out for any pair of ions in an ionic crystal. The only method which has been used so far to calculate the short range correlation potential between two ions in an ionic crystal is that based on the density functional theory of a uniform electron-gas. The implementation of this method presented originally by Gordon and Kim [8] was used in all the calculations to be described here. There is evidence reviewed in [5] that such calculations yield only the short range parts $V_{sXY}^{corr}(x_{XY}R)$ of the correlation energy whilst excluding the dispersion terms $V_{ab}^{disp}(x_{ab}R)$. The crystal dispersion energy $U_{disp}(R)$ was therefore computed separately using the methods described in section 3. Although the electron-gas method of calculating the short range correlation energy is approximate, the correlation corrections $V_{sXY}^{corr}(s_{XY}R)$ usually only constitute some 10% of the total short range term $V_{sXY}^{T}(x_{XY}R)$. Thus the errors in these corrections are sufficiently small that they do not affect the conclusions to be drawn from the calculations presented in this talk.

The equilibrium closest cation–anion separation (R_e) is just the value of R which minimises $U_L(R)$ and can therefore be predicted from knowledge of this function. The lattice energy, denoted D_e, which is the energy released on forming from the free ions in their electronic ground states the crystal having the equilibrium cation–anion separation R_e, is given by

$$D_e = -U_L(R_e) \tag{15}$$

The bulk compressibility, to be denoted B, can also be predicted from the function $U_L(R)$ through the definition

$$B = \{V\, d^2[U_L(R)]/dV^2\}_{R=R_e} \tag{16}$$

where V is the volume per formula unit CA_m. The expression (16) is evaluated through

$$B = (9k_v R_e)^{-1}\{d^2[U_L(R)]/dR^2\}_{R=R_e} \tag{17}$$

with k_v the constant relating V to R through $V = k_v R^3$

1. RELATIVISTIC EFFECTS FOR IONS OF HIGH ATOMIC NUMBER

1.1 Overview

Most quantum mechanical studies of the electronic structures of molecules and solids are based on the Schrödinger equation. Since the effects of special relativity are neglected in this equation, it does not provide an appropriate premise for investigating systems in which the velocities of the electrons are appreciable fractions of the velocity of light (c). Such high velocities arise not only for electrons in inner shell orbitals but also, in elements heavier than those of the third transition series, for valence electrons of low angular momentum [25].

The object of this section is to review in simple non-mathematical terms the evidence that relativity significantly modifies the behaviour of even the valence electrons in atoms and ions of high nuclear charge and then to study how these effects

are reflected in the properties of ionic crystals containing such ions. The role played by relativity in modifying the properties of a system can be elucidated by comparing the result of a calculation performed using the usual non-relativistic Schrödinger equation with that yielded from the calculation which differs only in using the relativistic version of quantum mechanics.

1.2 Relativistic Effects On Electrons In Atoms

1.2(i) One-electron atoms

In the relativistic quantum mechanics of a single electron, the stationary state wavefunctions corresponding to the allowed values of the energy are solutions of the Dirac equation [26,27]. For an electron subject to only an external electrostatic potential, this equation differs from the non-relativistic Schrödinger equation in two major respects. Firstly the relativistic (Dirac) kinetic energy operator involves 4×4 matrices. Secondly each relativistic orbital is a column vector with four rows and thus has four components unlike its counterpart in non-relativistic theory which has only a single component. Although the two lower components of a Dirac orbital play a crucial role in the mathematical formalism and must be considered in quantitative calculations, the mechanisms through which relativity modifies the properties of ionic crystals can be understood physically without considering these two components and focusing entirely on the upper two components. There are two upper components because an electron has a spin of one-half, electron spin being automatically incorporated in the Dirac formalism [26,27]. Thus an electron in the pure spin-up state has a wavefunction in which only the first upper component is non-vanishing, the second upper component being zero. Conversely the wavefunction for a spin-down electron has a vanishing first upper component with the second upper component being non-vanishing.

In the usual approximation of a stationary point nucleus having an atomic number Z, the Dirac Hamiltonian for a one-electron atom or ion has the same potential energy term $(-Z/r)$ as that in non-relativistic theory where r is the distance of the electron from the nucleus. Many properties of the relativistic orbitals of a one-electron atom are very similar to those of the standard non-relativistic atomic orbitals [27,28]. Thus the relativistic atomic orbitals designated as having s symmetry have no orbital angular momentum ($l = 0$) in the two upper components. The entire orbital has a total angular momentum (j) of one half which results from the coupling between the orbital and the spin angular momenta. For every non-relativistic atomic orbital having non-zero orbital angular momentum (l), there are two relativistic atomic orbitals, designated $\bar{l}$ and l, whose upper two components have the same value of l. These two orbitals have different values of j, equal to $l - 1/2$ and $l + 1/2$ respectively, which result from the coupling between the orbital and spin angular momenta. All bound relativistic atomic orbitals have an integral principal quantum number (n) which corresponds exactly to that in standard non-relativistic theory. Thus n can take the same numerical values as in non-relativistic theory, similarly restricts the allowed values of l and determines the number (n–l–1) of nodes in the radial part of the wavefunction entering the two upper components. There are $2j + 1$ degenerate orbitals which have the same radial wavefunctions and the same values of the quantum numbers n, l and j. These orbitals, said to constitute a subshell, differ only in the quantum number m_j that determines the z component of the total angular momentum j.

In a one-electron atom, all relativistic orbitals are more tightly bound than their non-relativistic counterparts in that their binding energies are greater and their mean radii are smaller [29]. Both the fractional increments in the binding energy and the contractions increase rapidly with increase of the nuclear charge (Z). This occurs simply because, for fixed quantum numbers n, l and j, increase of Z increases the electron velocity thereby enhancing the effects of relativity. For fixed Z the fractional increments in binding energy and contractions decrease with increasing total angular momentum j. The velocity of an electron in a given orbital is greater when the electron is close to the nucleus. The decrease of the electron density close to the nucleus as the j quantum number increases accounts for the reduction of the effect of relativity with increasing j. These modifications are said to arise from the direct relativistic effect [25,30]. This is the change in orbital properties which arises because the dynamics of the electron is intrinsically relativistic, this obeying the Dirac equation rather than the non-relativistic Schrödinger equation containing the same potential energy. The direct effect is very significant for s and $\bar{p}$ orbitals but is rather small for d, $\bar{f}$ and f orbitals [29]. It is hardly surprising that relativity is important for the $1s$ electron in heavy atoms because this is predicted to have a velocity equal to Z a.u. in non-relativistic theory. For a Z of 80 this is over half of the velocity of light which is 137 when measured in atomic units.

1.2(ii) Orbitals in many-electron atoms

The Dirac-Fock scheme for describing the electronic structure of a multi-electron atom is the relativistic analogue of the non-relativistic Hartree-Fock or orbital model of atomic structure [28,31]. In this scheme, it is usual to demand that the orbitals have the same spin and angular parts as those of a one-electron atom with the result that Dirac-Fock atomic orbitals can also be labelled by the four quantum numbers n, l, j and m_j. Hence only the radial parts of the orbitals in a multi-electron atom differ from their counterparts in a one-electron atom. It is also usual to demand that the radial parts of all the $2j + 1$ orbitals belonging to the same sub-shell are identical as in a one-electron atom. Orbitals having all these properties are said to have central field form. Each relativistic orbital can contain only a single electron so that a subshell of total angular momentum j can contain at most $2j + 1$ electrons.

In the relativistic description of a multi-electron atom, the operation of the direct relativistic effect causes the inner or core orbitals to be more contracted and tightly bound than their non-relativistic counterparts. The outermost orbitals in a multi-electron atom are subject not only to the direct relativistic effect but also to the indirect relativistic effect [25,30]. For an outer orbital, the indirect effect is the change in its properties which arises because the relativistic inner orbitals have become contracted compared with their non-relativistic counterparts through the operation of the direct relativistic effect. These contractions of the inner orbitals screen the outer electrons more effectively from the nuclear charge thereby acting to reduce the binding energies and increase the mean radii of the orbitals occupied by the outer electrons. Hence the indirect effect always acts to expand an orbital thereby opposing the direct effect which always acts to contract the orbital as in a one-electron atom.

One can separate the contributions made by the direct and indirect relativistic effects to the total relativistic modification of an orbital by performing the series of calculations [25] presented pictorially in Figure 2. In the full relativistic Dirac-Fock calculation for the gold atom, the $6s$ electron is considered to obey a Dirac equation containing the potential generated by a fully relativistic core. This full Dirac-Fock

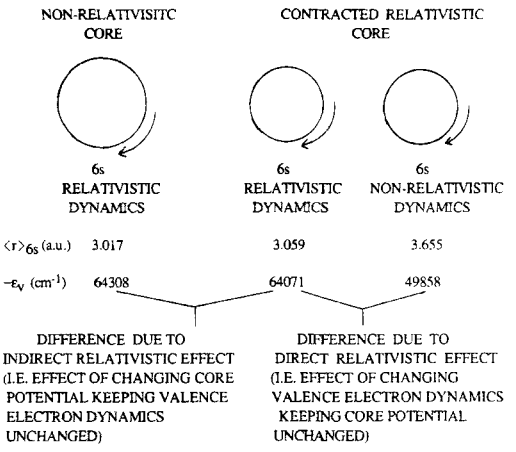

Figure 2 The direct and indirect relativistic modifications of valence electron behaviour.

calculation yields a 6*s* orbital which is considerably stabilized compared with that resulting from a standard non-relativistic Hartree-Fock calculation. Thus the relativistic 6*s* orbital obtained from the full Dirac-Fock computation has a mean radius of 3.059 a.u. and a binding energy of 64071 cm^{-1} compared with results of 3.701 a.u. and 48455 cm^{-1} from the entirely non-relativistic calculation. A computation in which the Dirac equation is solved for the 6*s* electron moving in the field of the core obtained from the entirely non-relativistic calculation yields an orbital having a mean radius of 3.017 a.u. and binding energy of 64308 cm^{-1} (Figure 2). This calculation of the 6*s* orbital differs from that in the full Dirac-Fock calculation solely in the substitution of the non-relativistic core for the relativistic core; in both calculations the dynamics of the 6*s* electron is treated relativistically by using the Dirac kinetic energy operator. Hence the difference between these two calculations gives a quantitative measure of the indirect relativistic effect originating from the change in the potential experienced by the 6*s* electron on account of the relativistic contraction of the core. The very close similarity of both the mean radii and binding energies of the 6*s* electron in the two calculations shows that its behaviour is only minimally influenced by the indirect effect which only very slightly destabilizes the 6*s* orbital. Comparison of the 6*s* orbital resulting from the full Dirac-Fock calculation with that derived by solving a non-relativistic Schrödinger equation for a 6*s* electron moving in the potential generated by the relativistic core gives a measure of the direct relativistic effect (Figure 2) because these two calculations use the same core potential and differ only in the dynamics of the 6*s* electron itself. The 6*s* orbital which results from solving the Schrödinger equation in the potential generated by the relativistic core is not only very significantly less tightly bound than the full Dirac-Fock 6*s* orbital but is also very similar to the 6*s* orbital resulting from the entirely non-relativistic calculation. This shows that the relativistic modification of the behaviour of the gold 6*s* electron originates almost entirely from the direct relativistic effect.

The behaviour of the gold 6*s* electron typifies that of valence *s* electrons in atoms of high nuclear charge. As for a one-electron atom, the large direct relativistic stabilizations of such valence *s* electrons arise because these have appreciable pro-

babilities of being found close to the nucleus where they move fast and are therefore significantly influenced by relativity.

Outer d ($j = 5/2$) electrons such the single $5d$ electron in lutetium [25] and the six $5d$ electrons in Pb^{++} [32] are destabilized by relativity, the orbitals resulting from a full Dirac-Fock calculation having larger mean radii and smaller binding energies than those yielded by the non-relativistic Hartree-Fock computation. Since the direct relativistic effect always acts to contract an orbital these destabilizations show that, for such orbitals, the indirect relativistic effect must outweigh the direct effect. A series of calculations of the type just described for gold shows that the magnitude of the indirect effect on an outer orbital increases with increase of its j quantum number [25] until for d orbitals ($j = 5/2$) this effect dominates the direct effect. It was similarly shown [25] that the magnitude of the direct effect decreases with increasing j to become small but not negligible for $\bar{d}$ and d electrons. Thus for d orbitals the situation is reversed compared with that for s orbitals where the direct effect dominates the indirect one. For relativistic p orbitals ($j = 3/2$) the calculations [25] show that the direct and indirect effects are comparable in magnitude with the result that the relativistic modifications of outer p orbitals are ofter rather small.

1.3 The Failure Of The Lowest Order Perturbation Description Of Relativity

For a one-electron atom, it is well known that to lowest order in the parameter Z/c the relativistic correction to the energy of the electron is given by taking the expectation value of a sum of operators each of which describes a different relativistic modification of its behaviour (see for example [27]). These expectation values are to be calculated using the non-relativistic wavefunction as would have been expected since this function is the unperturbed zeroth order state. This sum of operators contains three terms of which the spin-orbit coupling is perhaps the most well known. The two remaining terms are the mass-velocity operator originating from the velocity induced increase of the electron mass and the Darwin term describing a short range modification of the electron-nuclear attraction.

In the orbital description of a multi-electron atom, the leading relativistic correction to the energy of an electron is again given by taking the expectation value of a sum of operators using the non-relativistic wavefunction [33,34]. For an electron occupying orbital $|v\rangle$, the correction thus computed will be denoted $\varepsilon_v^{(1)}$. The terms in this sum of operators can be divided into two groups [33,34] which correspond to the perturbation theory descriptions of the direct and indirect relativistic effects. The first group consists of those terms arising for a one-electron atom, namely the mass-velocty plus spin-orbit coupling and Darwin terms originating from the electrostatic field generated by the nucleus, augmented by spin-orbit coupling and Darwin

Table 1 Comparison of Dirac-Fock and first order perturbation predictions of relativistic corrections to valence orbital energies[1]

		Au 6s	*Tl 6p*	*eka-Tl 7p*
Relativistic (Dirac-Fock) eigenvalue	ε_v	−64071	−46826	−58688
Exact Relativistic correction	$\varepsilon_v - \varepsilon_v^{NR}$	−15560	−4158	−17845
Perturbation correction	$\varepsilon_v^{(1)}$	−10587	−1884	+512

[1]All results in cm^{-1} taken from [35] (Au and Tl) and [36] (eka-Tl)

terms originating from the electrostatic field generated by the electrons in other orbitals. The latter field is evaluated using the description of these other orbitals provided by non-relativistic theory. The second group of operators, namely the perturbation theory description of the indirect relativistic effect, consists of the difference between the relativistic and non-relativistic descriptions of the electrostatic field generated by the electrons in other orbitals. If relativistic effects are small, the perturbation theory prediction ($\varepsilon_v^{(1)}$) of the relativistic correction to the energy of an orbital would naturally be expected to be the same as the difference ($\varepsilon_v - \varepsilon_v^{NR}$) between the orbital energy (ε_v) predicted from the Dirac-Fock calculation and that (ε_v^{NR}) computed using non-relativistic Hartree-Fock theory. For valence electrons in first and second row elements, it is has been shown [35] that the first order perturbation theory prediction $\varepsilon_v^{(1)}$ does indeed reproduce the difference $\varepsilon_v - \varepsilon_v^{NR}$.

Although first order perturbation theory works well for systems of low nuclear charge, one should not expect this to be capable of predicting the relativistic modification $\varepsilon_v - \varepsilon_v^{NR}$ if this is a significant fraction of the orbital energy ε_v^{NR}. The size of the nuclear charge for which the first order perturbation description of relativity breaks down can only be discovered by computing the differences $\varepsilon_v - \varepsilon_v^{NR}$ and then comparing these with the predictions $\varepsilon_v^{(1)}$. Three conclusions about the reliability of the first order perturbation description of valence electron behaviour have been drawn for such studies [35,36]. Firstly this description was shown to work reasonably well for the first series of transition elements. Secondly, for atoms heavier than copper but lighter than silver, it was shown to be incapable of making quantitatively accurate predictions although it is still of value qualitatively because its use introduces errors no greater than 10%. Thirdly it was shown that the first order perturbation theory breaks down for valence s and $\bar{p}$ electrons in elements heavier than those of the third series of transition elements. This is illustrated by the results in Table 1 which show that this approach loses one third of the relativistic correction to the energy of the gold 6s orbital and recovers less than a half of the correction to the energy of the $6\bar{p}$ orbital in thallium. For the superheavy element eka-thallium, this perturbation approach is not even capable of predicting the sign of the substantial relativistic stabilization of the $7\bar{p}$ orbital which, in this atom, contains the most loosely bound electron.

It might have seemed that the best way of rectifying the deficiences of the first order perturbation treatment of relativity would be to extend the perturbation treatment to higher orders. However this procedure not only generates a large number of operators whose expectation values are divergent but also produces divergent corrections to the orbitals. For the hydrogen atom all the calculations can be performed analytically and hence it was possible to show [37,38] that these divergencies cancel to yield the correct finite result for the relativistic modification of the energy. However for both molecules and multi-electron atoms analytic expressions for the Hartree-Fock orbitals are not available and hence for these systems the divergences arising in higher order perturbation descriptions of relativity cannot be handled by the techniques used in [37,38]. Thus attempts to use high order perturbation descriptions of relativity in both molecules and multi-electron atoms would appear to be unpromising.

1.4 The Relativistic Integrals Programme (RIP)

The breakdown of the first order perturbation treatment of relativistic effects in atoms of high nuclear charge coupled with the divergence difficulties arising in higher orders of perturbation theory shows that the relativistic electronic structures of solids and

molecules are best investigated by working directly with the Dirac equation and building the multi-electron wavefunction from fully relativistic orbitals each of which has four components. The Relativistic Integrals Programme (RIP) was therefore developed [22–24] to calculate exactly the energy of such a relativistic wavefunction for any diatomic system. Hence the programme can be used either to compute a relativistic wavefunction for an isolated diatomic molecule [23,39,40] or to calculate the uncorrelated short range interactions $V^0_{sXY}(x_{XY}R)$ for pairs of ions in ionic crystals. It is the latter facility that is the key that enables one to investigate ab-initio the properties of such crystals even when they contain the heaviest ions. It should be emphasized that the potential $V^0_{sXY}(x_{XY}R)$ computed using the RIP programme is exact once the wavefunctions of the two ions X and Y are given. Hence such computations with the RIP programme do not contain any of the uncertainties that arise if these potentials are calculated using density functional theory. Moreover as discussed in section 4, the RIP results can therefore be used to test the accuracy of the latter approach.

The RIP programme requires that the radial parts of the four component wavefunctions of the one-electron orbitals used to construct the multi-electron wavefunction for the pair of interacting ions are represented in the numerical form generated by the Oxford atomic Dirac-Fock programme. However since each of the wavefunctions of the individual ions is generated from a run of this programme, every orbital has the required numerical form. Furthermore since the orbitals of the two ions are generated by solving the Dirac-Fock equations numerically, these orbitals are automatically the true Dirac-Fock orbitals for the ions. Hence studies of ionic crystals using the RIP programme avoid any of the uncertainties concerning the quality of the basis set that would arise if the standard techniques of non-relativistic quantum chemistry were used, an infinite basis being in principle necessary to generate orbitals equivalent to those obtained from a numerical calculation. In practice an inconveniently large basis would be needed for solids containing heavy ions, a problem entirely circumvented in RIP calculations. Thus it is known (see for example [5]) that large basis sets are needed to compute accurately the interaction energy between even two light ions using the techniques of non-relativistic quantum chemistry. The use in the RIP programme of numerical orbitals for the ions also avoids the further problems which arise when one attempts to extend the non-relativistic quantum chemistry techniques to relativistic calculations. These problems which have been extensively discussed elsewhere [41] will not be considered here because they are entirely circumvented in studies of ionic solids using the RIP programme.

1.5 Relativistic Modifications Of Crystal Properties

1.5(i) Modifications of inter-ionic potentials

The short range interaction $V^0_{sXY}(x_{XY}R)$ between two ions neither having any unpaired electrons has always been found to be repulsive except for a few anion–anion interactions which are discussed in detail elsewhere [4,5]. These repulsions ultimately originate from the Pauli principle which prevents two electrons of the same spin from occupying the same orbital. Hence when two such orbitals on different ions overlap, the electronic structure can be envisaged in terms of two orthogonal orbitals both formed as linear combinations of the two original overlapping orbitals. This orthogonalization introduces an extra node into one of the orbitals which increases its kinetic energy thus accounting for the repulsion.

The outermost orbital in the Pb^{++} ion, namely the 6*s* orbital, is significantly contracted by relativity, the relativistic orbital having a mean radius of 2.233 a.u. compared with one of 2.506 a.u. for the non-relativistic 6*s* orbital. One therefore expects the short range repulsion between two Pb^{++} ions to be reduced by relativity provided that the inter-ionic separation is not so short that the overlap of the 6*s* orbitals ceases to make the dominant contribution to this repulsion. Computations using the RIP programme do indeed confirm that this repulsion is significantly reduced by relativity. The data presented in Table 2 taken from [32] compare both the short range Pb^{++} ..F^- and Pb^{++} ..Pb^{++} potentials calculated relativistically with the exactly corresponding non-relativistic potentials. The non-relativistic results were calculated using the same computer programmes and in exactly the same way as the relativistic results except that the programmes were run using an artificially large value for the velocity of light, greater by a factor of 1000 than the true value of 137.0373 a.u. used in the relativistic calculations. For closed shell systems, this technique of performing relativistic calculations with a greatly increased value for the velocity of light is known to reproduce exactly the results of non-relativistic computations [42,43]. The influence of the environment on the ion wavefunctions was described by using the best of the models described in section 2. Although this model may be improved in future work, the magnitudes of the relativistic effects as derived from the differences between the relativistic and non-relativistic calculations will not be significantly changed by any possible future improvements in this model because the same model was used in all the calculations. Furthermore these calculations show that the crystalline environment scarcely affects the Pb^{++} wavefunctions which therefore hardly differ from those of an isolated Pb^{++} ion. For the form of PbF_2 having the fluorite structure with closest Pb^{++} ..F^- separation R, the short-range Pb^{++} ..Pb^{++} repulsions calculated for the distances $2\sqrt{(2/3)}R$ which separate the closest pairs of Pb^{++} ions are seen (Table 2) to be reduced by relativity by factors as large as three.

Since the wavefunction of the fluoride ion is essentially unaffected by relativity, the relativistic modifications (Table 2) of the short-range Pb^{++} ..F^- interaction are determined by the interplay between the relativistic contraction of the 6*s* orbital and the expansion, originating from the indirect relativistic effect, of the Pb^{++} 5*d* ($j = 5/2$) orbital. For this latter orbital the dominance of the indirect over the direct relativistic effect explains why its mean radius (1.300 a.u.) is larger in relativistic theory than that (1.259 a.u.) in the non-relativistic description. At larger values of R, the overlap between the orbitals of the F^- ion with the Pb^{++} 5*d* orbitals is less important than that with the relativistically contracted 6*s* orbital thereby accounting for the relativistic reduction of the short-range Pb^{++} ..F^- repulsion for $R > 4.0$ a.u.

Table 2 The influence of relativity on the uncorrelated short range inter-ionic potentials in cubic lead fluoride[1,2,3]

$V^0_{sPb++Pb++}(2\sqrt{(2/3)}\,R)$			$V^0_{sPb++F-}(R)$	
R	*relativistic*	*non-relativistic*	*relativistic*	*non-relativistic*
4.0	0.00432	0.01318	0.07767	0.07533
4.5	0.00085	0.00306	0.03419	0.03507
4.75	0.00040	0.00151	0.02313	0.02434

[1] Distances R and energies in atomic units (a.u.).
[2] Computed using the RIP programme using ion wavefunctions calculated using the model environmental potentials (19) and (22).
[3] Relativistic results taken from [4] and non-relativistic results from [32].

Table 3 Relativistic modifications of the properties of cubic lead fluoride[1]

	Uncorrelated from $U_L^0(R)$ equation (11)		*Correlated plus damped dispersion $U_L(R)$ equation (14)*		*expt*[2]
	Rel	*NR*	*Rel*	*"NR"*[3]	
D_e (kJ mole^{-1})	2288	2257	2433	2406	2491
R_e (a.u.)	5.06	5.11	4.866	4.91	4.861
$B(10^{12}\text{Nm}^{-2})$	5.20	5.06	6.56	6.14	6.53

[1]Relativistic results (denoted Rel) from [4] and Non-relativistic results (denoted NR) from [32].
[2]For sources of experimental data see [4] or [5].
[3]Non-relativistic calculation of uncorrelated short range potentials $V_{sXY}^0(x_{XY}R)$ and short range correlation terms $V_{sXY}^{corr}(x_{XY}R)$ but relativistic (from experimental polarizabilities) dispersion energy $U_{disp}(R)$.

(Table 2 and Table 1 of [32]). Since the Pb^{++} 5*d* orbital has a much smaller mean radius than the 6*s* orbital, one can expect the relative importance of the overlap of the F^- ion orbitals with the 5*d* orbitals compared with the 6*s* orbitals to increase as *R* decreases. The relativistic enhancement (Table 2) of the short range Pb^{++} ..F^- repulsion at R = 4.0 a.u. can be attributed to the increase of this relative importance, the contribution to the relativistic modification of this potential originating from the enhancement of the repulsion caused by overlap with the relativistically expanded 5*d* orbitals outweighing the reduction of that originating from the overlap with the relativistically contracted 6*s* orbital.

1.5(ii) Modifications of bulk crystal properties

The degree to which the relativistic modifications of the inter-ionic potentials are reflected in the cohesive properties of crystals is elucidated by comparing the exactly analogous relativistic and non-relativistic predictions of the lattice energy (D_e), equilibrium closest cation–anion separation (R_e) and bulk compressibility (B). The results of such a comparison [32] for the cubic form of lead fluoride are summarized here by the results assembled in Table 3.

Comparison of the results in the first two columns of Table 3 shows how relativity modifies the predictions obtained from the expression (11) for the crystal cohesion that is derived by considering only the uncorrelated short range potentials. The relativistic reductions of both the uncorrelated short range Pb^{++} ..Pb^{++} and Pb^{++} ..F^- interactions cause the crystal cohesion to be slightly increased by relativity. A more detailed examination presented elsewhere [32] shows that the reduction of the uncorrelated short range Pb^{++} ..Pb^{++} potential contributes roughly half of the total relativistic stabilization. Although the fractional relativistic modification of the Pb^{++} ..Pb^{++} potential is much greater than that of Pb^{++} ..F^- interaction, this is not reflected to the same extent in the modification of the crystal cohesion because the smallest Pb^{++} ..Pb^{++} separation is greater than the closest cation–anion separation R by a factor of $2\sqrt{(2/3)}$.

It has been shown elsewhere [32] that introduction of the short range correlation potentials $V_{sXY}^{corr}(x_{XY}R)$ leaves essentially unchanged the relativistically induced changes in D_e, R_e and B that are predicted when only the uncorrelated short range interactions are included. Naturally the crystal cohesion predicted by both the non-relativistic and relativistic calculations is increased by introducing these correlation terms. A full calculation [4] of the crystal cohesion, which yields results in excellent

agreement with experiment, must include the dispersion energy $U_{disp}(R)$ calculated taking account of its damping [6,7] that arises from the overlap of the ion wavefunctions. The calculation of the dispersion energy requires knowledge of the dispersion coefficients of which the most important are the dipole-dipole or $C_6(XY)$ dispersion coefficients. For lead fluoride these had to be calculated [4] from the static polarizabilities of the ions which were deduced [44] from the experimentally measured values of the crystal refractive indices. The values of the dispersion coefficients thus derived naturally include the effects of relativity since the velocity of light is finite in the real world. However the non-relativistic dispersion energy of the crystal is not available because it cannot be derived from this procedure. Hence it is not possible to report a completely non-relativistic analogue of the relativistic calculation which includes the dispersion. However, columns 3 and 4 of Table 3 show that the difference in the crystal cohesion predicted from the relativistic and non-relativistic calculations including only the short range potentials remains unchanged if the same relativistic dispersion energy is introduced into both these two calculations. The calculation of the dispersion energy $U_{disp}(R)$ is described in detail in section 3.

It has been shown that relativity reduces the uncorrelated short range Pb^{++} ..Pb^{++} interaction by a factor of three. Although the influence of relativity on the properties of perfect PbF_2 crystals is not so dramatic as that on the inter-ionic potentials because the distances between the Pb^{++} ions are quite large, the very substantial relativistic modification of the short-range Pb^{++} ..Pb^{++} repulsion shows that it would be highly inadvisable to attempt to describe crystals containing such heavy ions by using non-relativistic calculations. Furthermore the relativistic reduction of this repulsion can be expected to become more important for the energetics of crystal defects involving interstitial Pb^{++} ions where smaller internuclear separations arise. These results can be expected to be typical of those for systems containing such heavy ions.

2. ENVIRONMENTALLY INDUCED MODIFICATIONS OF ION WAVEFUNCTIONS

2.1. The Physics Of The Environment

Each electron of an ion in an ionic crystal interacts with the environment generated by the presence of the other ions and their attendant electrons [45]. It should be expected that any modifications of the ion wavefunctions caused by such interactions will influence the inter-ionic potentials [4,19,24]. The object of this section is to describe the extent and mechanisms through which both the inter-ionic potentials and individual ion polarizabilities are modified by these interactions with the crystalline environment. The modifications [44–48] of the ion polarizabilities are interesting not only in themselves but also because, as discussed in section 3, any such changes are further reflected in the inter-ionic dispersion coefficients [4,49,50]. These coefficients govern the dispersive attractions between the ions.

The fundamental theory of the influence of the crystalline environment on the ion wavefunctions is developed by assuming that the total wavefunction for all the N_{cr} electrons in the crystal can be written as an anti-symmetrized product of individual ion wavefunctions which one demands are optimal for the crystal geometry specified by the closest cation–anion separation R. In the approximation that electron correlation is neglected, this reduces to writing the crystal wavefunction as an anti-symmetrized product of individual ion wavefunctions constructed using the orbital approxi-

mation. The optimum orbitals are determined by demanding that the total crystal energy $E_{cr}(R)$ is stationary with respect to those variations of the orbitals which can be realized within the constraints that all the orbitals remain normalized and that those belonging to the same ion remain orthogonal. The optimum orbitals belonging to a given ion (a) are then found to be eigenfunctions of an operator which is analogous to that arising in the Hartree-Fock or orbital theory of atomic electronic structure. Thus this Fock like operator contains all the terms which arise in the Hartree-Fock description of the isolated ion a augmented by an additional potential, to be denoted $F_{env}(\mathbf{r}_a;R)$, which originates from all the other ions in the crystal. Clearly for an electron belonging to ion a, this additional potential is a function of the position vector $\mathbf{r}_a$ defined relative to the nucleus of ion a. The environmental potential $F_{env}(\mathbf{r}_a;R)$, which will certainly be non-local unless it is approximated, depends on the crystal geometry and therefore carries the label R.

It is useful to decompose the environmental potential $F_{env}(\mathbf{r}_a;R)$ acting on an electron on ion a into three contributions [4,45]. The first of these is that which would arise if all the ions b other than the ion a containing the electron under consideration were replaced by point charges of magnitude $Z_b - N_b$. Thus the first contribution is that generated by a point charge lattice. The second contribution is the correction that arises when the purely electrostatic potential generated by the electrons on ions b is calculated more realistically taking account of the extension in space of the charge distribution generated by these electrons. The potential generated as the sum of these first two contributions ignores any effects which arise from the exchange of electrons on ion a with those belonging to the neighbouring ions b. There are two terms in the environmental potential that arise from such exchange and their sum constitutes the third contribution to $F_{env}(\mathbf{r}_a;R)$. The first of the two terms originates from the Pauli principle and involves primarily the kinetic energy of the electrons and their attraction to the nuclei. The second term is that part of the total electron-electron repulsion that involves the exchange of the considered electron of ion a with electrons belonging to neighbouring ions b. Both these terms are only non-zero if the orbital containing the electron on ion a has a non-negligible overlap with one or more occupied orbitals of the neighbouring ions.

In any exact theory of the environmental potential, each of the two terms in the third contribution to $F_{env}(\mathbf{r}_a;R)$ would appear as a non-local operator, that is one which cannot be defined solely as a numerical value at each point in space. By contrast a local operator has a definite numerical value at each point in space that is the same regardless of the wavefunction on which it may act, the electrostatic potential $-Z_a/r_a$ generated by a nucleus (a) providing a simple example. However, physically the first term in this third contribution constitutes a repulsive potential acting on an electron belonging to ion a in regions of space in which the electron density on neighbouring ions does not vanish. This repulsion ultimately originates from the Pauli principle which prevents an electron on ion a from entering an orbital of ion b that is completely filled with electrons. This principle forces the wavefunction of ion a to be orthogonal to these occupied orbitals of ion b which introduces an extra node into the orbital on ion a thereby increasing its kinetic energy. This increase in the kinetic energy of the electron on ion a in spatial regions where the density of electrons on neighbouring ions is non-vanishing is the primary cause of the repulsion originating from the first term. The second term in the third contribution to $F_{env}(\mathbf{r}_a;R)$, namely that portion of the electron-electron repulsion that originates from exchange of an electron on ion a with

those on neighbouring ions, effectively acts as an attractive potential in spatial regions in which the electron density of these neighbours is not negligible. However the repulsion originating through the operation of the Pauli principle has a greater magnitude than the attractive exchange component and consequently the third contribution to $F_{env}(\mathbf{r}_a;R)$ constitutes overall a repulsive potential.

The derivation of explicit forms for the environmental potential is at a sufficiently early stage of development that it would appear advisable to demand that all the ion orbitals in the crystal have the same central field form as those of the free ions. As discussed in section 1.2(ii), this means that the angular and spin parts of the orbitals are the same as those in a one-electron atom but that the radial parts of the orbitals differ from those of the free ions. It is useful to consider expanding the environmental potential in a series in which spherical harmonics are used to describe its angular variation [4,45]. Such an expansion takes the form

$$F_{env}(\mathbf{r}_a;R) = F^{(0)}_{env}(r_a;R) + \ldots \tag{18}$$

The first term of this expansion, which is the only one required here, is independent of any angular variables and thus depends only on the radial distance r_a of the electron from the nucleus of ion a and constitutes the spherically symmetric part of the environmental potential. This is denoted by the superscript 0. This spherically symmetric part can be generated by averaging the full potential $F_{env}(\mathbf{r}_a;R)$ over the two angular variables entering the position vector $\mathbf{r}_a$. The sum of all the unwritten terms in (18) describes the angular variation of $F_{env}(\mathbf{r}_a;R)$. It has been shown [4] that each of these unwritten terms contributes zero to the total energy of all the electrons on ion a in a crystal provided that all the orbitals belonging to ion a not only have central field form but also are either completely filled with electrons or are totally unoccupied. Thus computation of the ion orbitals retaining only the spherically symmetric part of the environmental potential will yield orbitals which have the central field form that is needed to show that the unwritten terms on the right hand side of (18) do not contribute to the energy. Hence for crystals composed of closed shell ions, retention of only the spherically symmetric part $(F^{(0)}_{env}(r_a;R))$ of $F_{env}(\mathbf{r}_a;R)$ yields a theory which is internally self-consistent.

The derivation of explicit forms for even the spherically symmetric part $F^{(0)}_{env}(r_a;R)$ of the environmental potential is at a sufficiently early stage of development that only purely local representations of $F^{(0)}_{env}(r_a;R)$ will be considered further. In computations of ion wavefunctions using the Oxford Dirac-Fock [21] or any other programme for generating atomic wavefunctions, the appropriate local approximation to the function $F^{(0)}_{env}(\mathbf{r}_a;\ R)$ is added to the term describing the interaction of each electron with the nucleus of ion a. Such computations yield ion wavefunctions which are adapted to the crystalline environment in that the radial wavefunctions are optimal for the latter and differ from those of the free ions. The resulting ion wavefunctions being built from orbitals having central field form can therefore be used as input to the computation using the RIP programme of the uncorrelated short range interactions $V^0_{sXY}(x_{XY}R)$.

Clearly each of the three contributions to the total environmental potential $F_{env}(\mathbf{r}_a;R)$ which were described above in the third paragraph of this subsection can also be expanded in a series of the type (18). The spherically symmetric part $(F^{(0)}_{env}(r_a;R))$ of the total environmental potential is the sum of the spherically symmetric parts of these three contributions.

2.2 *The Environmental Potential Acting On Anion Electrons*

2.2(i) *Basic physics and formulation of a model*

Three successive approximations to the spherically symmetric part $F_{env}^{(0)}(r_A;R)$ of the environmental potential acting on an electron belonging to an anion, designated A, are generated by considering in turn the three contributions to $F_{env}(\mathbf{r}_a;R)$ introduced in the last subsection. Each of these successive approximations is depicted in Figure 3, a local approximation being used for the third contribution.

The first approximation to $F_{env}^{(0)}(r_A;R)$, appearing as the curve (1) in Figure 3, arises from the first contribution to $F_{env}(\mathbf{r}_a;R)$ which is that generated by a point charge lattice. The spherically symmetric component of the potential originating from a point charge lattice is the same as the potential produced by the charge distribution generated by the following averaging procedure. For all distances r_s from the nucleus of ion A all the point charges arising at the distance r_s are averaged over the surface of a sphere of radius r_s. The resulting potential is constant from the nucleus of ion A ($r_A = 0$) to the distance R equal to the closest cation–anion separation because, for these distances, the electron is inside all the spherical shells of charge, the potential inside a spherical shell of charge being constant. This constant potential is attractive for an anion electron because the closest shell contains the positive charge generated by averaging the positions of the closest neighbouring cations each approximated as

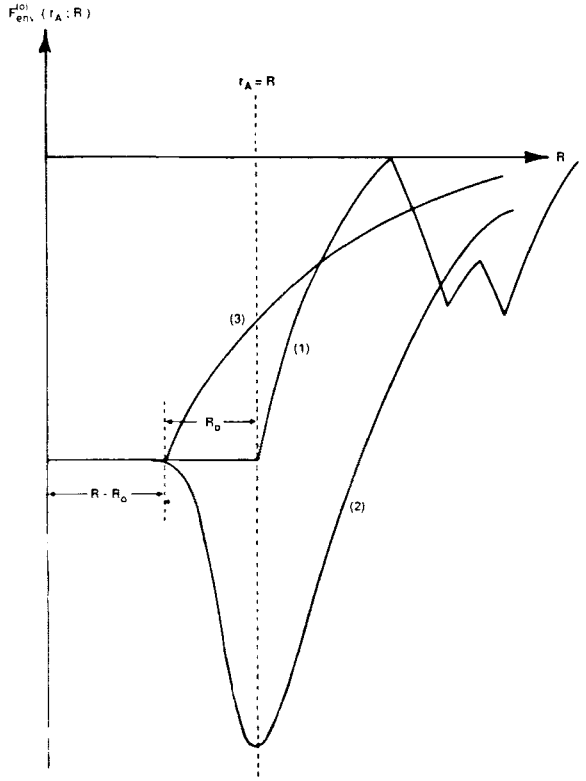

Figure 3 The spherically symmetric part of the environmental potential acting on an anion electron.

a point charge. For distances r_A greater than R, the magnitude of this potential decreases because the potential outside a spherical shell of charge is the same as if the charge were placed at the centre ($r_A = 0$). The smaller oscillations in the potential (1) at larger distances r_A are associated with distances corresponding to non-nearest neighbour separations. Clearly an anion electron subject to an additional attractive potential well of the type (1) will be both more tightly bound than in the free anion and have a charge distribution contracted compared with that in the free anion.

Treating the potential generated by the electrons on the nearest cation neighbours more realistically by taking account of the actual spatial extensions of these cation orbitals but neglecting exchange with electrons occupying these orbitals yields the potential labelled (2) in Figure 3. This is the spherically symmetric part of the sum of the potential (1) and the correction generated by the more realistic treatment of the closest cations. The main feature of this potential compared with that (1) is the large attractive well centred at a distance R. This well originates from the attraction with all the n_{CA} nuclei in the first shell of neighbouring cations; the spherical average of this potential being that due to a total charge $n_{CA}Z_C$ uniformly distributed over a sphere of radius R.

The potential labelled (3) in Figure 3 is a schematic representation of that $F_{env}^{(0)}(r_A;R)$ produced by adding to the potential (2) the effects generated by exchange with the electrons on the neighbouring ions. The purely electrostatic repulsion generated by the electrons on the neighbouring ions has already been included in the potential (2) so that the additional repulsion shown by potential (3) originates essentially from the increase in the kinetic energy experienced by an electron in spatial regions where the density of electrons on neighbouring ions is non-zero as discussed in the previous sub-section. The depiction of the total potential in a graph showing the numerical value of $F_{env}^{(0)}(r_A;R)$ at a distance r_A from the centre of the nucleus of ion A implies that a local approximation has been used for the totality of effects originating from the exchange. It is clear that this third contribution, whether approximated by a local potential or treated more accurately as a non-local operator, will act to contract anions thereby reinforcing the same effects generated by the point charge lattice (potential (1)).

The development of ab-initio computations of the properties of ionic solids is at a sufficiently early stage of development that it is reasonable to use the simplest local approximation to the potential (3). A simple yet physically realistic model potential was developed [4] by noting that, for values of r_A sufficiently small that the density of electrons on neighbouring ions is negligible, the total potential $F_{env}^{(0)}(r_A;R)$ will not differ significantly from that generated by a point charge lattice. The largest value of r_A for which the neighbouring ion electron density is still negligible will be defined to be R–R_0. For values of r_A greater than $R - R_0$, the total potential should increase reaching zero asymptotically as shown by the potential (3) in Figure 3. A model potential $F_{env}^{(0)}(r_A;R)$ having these properties is

$$F_{env}^{(0)}(r_A;R) = -\phi_{envA}/R \qquad r_A \leqslant R - R_0 \tag{19a}$$

$$F_{env}^{(0)}(r_A;R) = -k_{envA}/r_A \qquad r_A \geqslant R - R_0 \tag{19b}$$

The positive constant ϕ_{envA} is chosen [4] such that (19a) reproduces the environmental potential generated by the point charge lattice, the explicit factor of R^{-1} being introduced to make ϕ_{envA} independent of the crystal geometry as defined by the closest cation–anion separation R. The constant k_{envA} in (19b) is chosen to make the potential

$F^{(0)}_{env}(r_A;R)$ continuous at $r_A = R - R_0$ [4]. Although the particular functional dependence on r_A of the potential (19b) was chosen merely for computational convenience, (19b) has the correct qualitative physical behaviour in as much as it increases smoothly towards zero from the value given by (19a). The criterion that the density of electrons on neighbouring ions is negligible at distances smaller than $R - R_0$ from the nucleus of the anion A shows that R_0 should be chosen to be approximately equal to the radius of the cation C. A method for generating from the mean radius and eigenvalue of the outermost cation orbital a value for R_0 closely approximating the cation radius has been presented elsewhere [4].

2.2(ii) Test of model anion environmental potential for sodium fluoride

The model, introduced in the last subsection, for describing the influence of the crystalline environment on anion wavefunctions has been tested [4] for sodium fluoride choosing R to be 4.5 a.u. which is close to the experimental R_e value of 4.38 a.u.. These tests consisted of comparing both the wavefunctions of the individual ions and the crystal cohesion predicted from them using the simplest approximation retaining only the Madelung term and the uncorrelated short range repulsion between each Na^+ ion and its closest F^- neighbours. In this approximation the expression (11) for the cohesive energy reduces to

$$U^0_L(R) = -M/R + 6V^0_{sNa^+F^-}(R) + E^{Na^+}_{Re}(R) + E^{F^-}_{Re}(R) \qquad (20)$$

The wavefunction of the free Na^+ ion was used in all the calculations whose results are presented in Table 4, so that $E^{Na^+}_{Re}(R)$ is zero. Hence the rearrangement energies reported in the third line of numerical data in this table originate from just the fluoride ion.

The results presented in the first column of Table 4 were derived using the wavefunctions of the free fluoride ion. These results can be compared with those reported in the second column which were derived by computing the F^- ion wavefunction using the description of the environment provided by the purely elec-

Table 4 Influence of fluoride on wavefunction on the binding of NaF at R = 4.5 a.u.[1]

	Description of environmental potential used to compute wavefunction[2]			
	free	*exact coulomb*[3]	*point coulomb*[4]	*model (19) + (22)*[5]
$<r>_{2pF^-}$	1.257	1.275	1.245	1.224
α_{F^-}	15.1		10.8	6.95[6]
$E^I_{Re}(4.5)$	0	9	3	10
$V^0_{sC.A}(4.5)$	23	26	21	17
$U^0_L(4.5)$[7]	−879	−853	−893	−905

[1] All results from [4] excepting F^- ion polarizabilities α_{F^-} in a.u. taken from [47] and [52]; $<r>_{2pF^-}$ in a.u. and all energies in kJ mole^{-1}.

[2] All results derived using free ion Na^+ wavefunction.

[3] Electrostatic potential originating from the full charge distribution of six closest Na^+ ions plus point charge description of remainder of lattice; potential (2) of Figure 3.

[4] Electrostatic potential generated by a point charge lattice; potential (1) of Figure 3.

[5] Full environmental potential as modelled by relations (19) and (22); potential (3) of Figure 3.

[6] Deduced [47] from experimental polarizability of NaF crystal by subtracting known constant polarizability of Na^+.

[7] Positive crystal binding energy equals the magnitude of $U^0_L(4.5)$.

trostatic potential (2) in Figure 3 which neglects the effects originating from exchange with electrons on neighbouring ions. In this test calculation [4] the computational machinery incorporated in the RIP programme was used to compute exactly the electrostatic potential originating from the closest neighbouring Na^+ ions thereby taking account of the finite spatial extensions of their electronic charge distributions. The F^- ion 2p orbital computed using this environmental potential is more expanded than that of the free F^- ion as shown by its greater mean radius (see Table 4). This expansion is caused by the deep attractive well centred at $r_A = R$ which originates from the electrostatic potential generated by the nuclei of the neighbouring Na^+ ions (see potential (2) of Figure 3). This expansion of the F^- ion 2p orbitals causes the short range repulsion $V^0_{sNa^+F^-}(R)$ to be even greater than that between a free F^- ion and a free Na^+ ion. In any calculation which does not use free ion wavefunctions, the rearrangement energies of the ions act to reduce the binding energy of the crystal. If a physically correct model of the crystalline environment has been used, the rearrangement energy $E^T_{Re}(R)$ is more than offset by the decrease in the short range repulsions to yield a crystal cohesion increased relative to that predicted using free ion wavefunctions. The incorrectness of the potential (2) of Figure 3 is manifested by the fact that it predicts an increased short range repulsion which reinforces the effect of the rearrangement energy to predict a crystal cohesion less than that derived using free ion wavefunctions. The quantum mechanical variation principle shows that one has used a worse wavefunction for the entire crystal if the energy is raised which provides strong evidence that the potential (2) is incorrect. It has already been pointed out that the potential (2) is qualitatively incorrect because the well in this potential centred at $r_A = R$ disappears when the effects of exchange with electrons on neighbouring cations are introduced to produce the potential (3). This shows that the expansion of the F^- ion wavefunction generated by using the potential (2) is entirely spurious. Thus it can be concluded both from the mathematical argument based on the variation principle and from the physical reasoning that it is incorrect to use the potential (2).

The representation of the crystalline environment by either the potential (1) due to a point charge lattice or the local approximation (19) ((3) of Figure 3) yields results very different from those generated by using the potential (2). Thus the 2p orbital of the F^- ion is found (Table 4) to be contracted relative to that of the free ion if the F^- ion wavefunction is computed using either of the representations (1) and (3) of Figure 3. The data in Table 4 show that the reduction of the short range repulsion $V^0_{sNa^+F^-}(R)$ resulting from these contractions more than outweighs the F^- ion rearrangement energy thereby increasing the predicted crystal cohesion. It should be noted that the short range repulsion enters the expression (20) for $U^0_L(R)$ with a factor of six as opposed to that of unity for the rearrangement energy so that a reduction of the former more than outweighs an equal increase in the latter. Both the orbital contraction and increased cohesion that result from introducing the point charge environmental potential (1) are comparable to the further contraction and increased binding arising on passing from using this potential to using the local representation (19) of the full environmental potential.

The polarizabilities of ions in crystals are of interest not only for the insights they yield into the electronic structures of ions but also because they govern the optical and dielectric properties of polar solids [51] as well as entering the most reliable semi-empirical method for calculating inter-ionic dispersive attractions. There has been much interest in elucidating the mechanisms through which the environment of an ion in a crystal might modify the ion polarizability. It was pointed out by Mahan [45] that

the purely electrostatic potential (curve (1) of Figure 3), constituting an attractive well, would be expected to increase the binding of anion electrons thereby reducing anion polarizabilities. This suggestion has been confirmed by accurate ab-initio quantum chemistry calculations [46–48] in which account was taken of electron correlation. Thus the results presented in the second line of Table 4 show that polarizability computed for a fluoride ion in a point charge lattice having an R of 4.38 a.u. equal to the experimental R_e of NaF is significantly reduced compared with that calculated [52] for a free fluoride ion. Changing the representation of the crystalline environment from a point charge lattice to a lattice composed of actual ions including their attendant electrons would be expected to reduce anion polarizabilities still further. Such reductions are to be predicted because the overlap of the anion orbitals with those of neighbouring ions generates through the Pauli principle an additional repulsive potential acting on an anion electron which will tend to compress the anion. The difference between the potentials (1) and (3) of Figure 3 shows a local representation of the spherically symmetric part of this additional compressive potential. For a fluoride ion in NaF the polarizability of 10.8 a.u. in the point charge lattice is further reduced to the experimentally deduced value of 6.95 a.u. in the actual crystal where the electrons are naturally subject to the full environmental potential [47]. Thus both point charge electrostatics and overlap effects reduce the polarizability of the fluoride ion by roughly the same fractions. Similarly the contractions of the F^- ion 2p orbitals induced by these two effects generate comparable reductions in the uncorrelated short range repulsion ($V^0_{sNa+F^-}(R)$) with the six closest neighbouring sodium ions.

2.3 *The Environmental Potential Acting On Cation Electrons*

The function (3) in Figure 4 shows a schematic representation of a local approximation to the spherically symmetric part ($F^{(0)}_{env}(r_C;R)$) of the potential acting on a cation electron. The quantity r_C denotes the distance of an electron occupying a cation orbital from the nucleus of the cation C. The potential $F^{(0)}_{env}(r_C;R)$ can be decomposed into that arising from a point charge lattice, the correction generated by taking account of the spatial extensions of the orbitals on neighbouring anions plus the repulsion originating from exchange with electrons belonging to these neighbours. The function labelled (1) in Figure 4 shows the spherically symmetric part of the potential generated by the point charge approximation to all the ions other than the cation C under consideration. This point charge lattice potential differs from that discussed in the last subsection (2.2) for an anion electron solely in having the opposite sign. For distances r_C less than the closest cation–anion separation R, this potential acting on a cation electron is constant because it can be regarded as arising from the spherically symmetric shells of charge generated as the spherical average of the point charge lattice. This potential is destabilizing for a cation electron because the closest neighbouring ions are negatively charged. The potential (2) of Figure 4 is generated by adding to that (1) the correction arising from the spatial extension of the electron densities on the closest neighbouring anions whilst neglecting exchange with electrons on these anions. For the reasons already discussed in section 2.2, it is the attraction of a cation electron for the nuclei of the closest anion neighbours which is responsible for the deep well centred at the distance R in the potential (2) of Figure 4. The spherically symmetric part ($F^{(0)}_{env}(r_C;R)$) of the total environment potential is generated by adding to the potential (2) the repulsion experienced by a cation electron in spatial

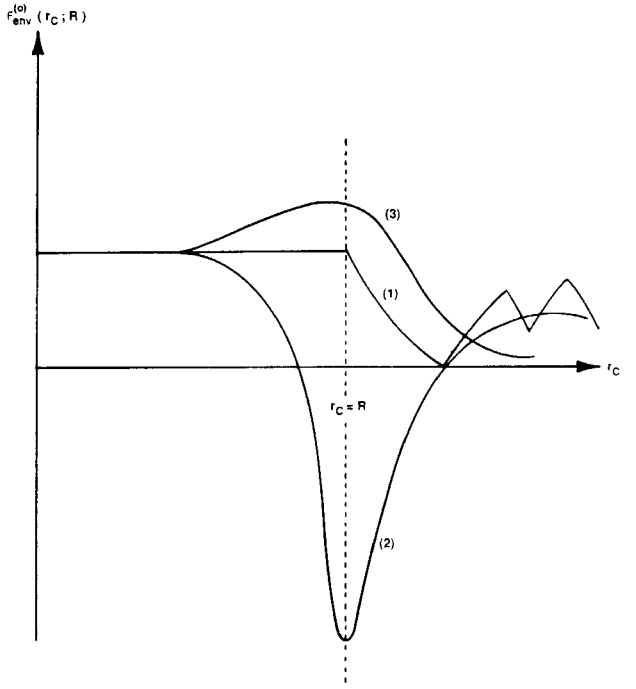

Figure 4 The spherically symmetric part of the environmental potential acting on a cation electron.

regions where the anion electron density is non-zero. The curve labelled (3) in Figure 4 is generated [45] by adding to the curve (2) this repulsion which originates because effects due to the Pauli principle outweigh the exchange contribution to the inter-ionic electron-electron interaction. This curve (3) shows no traces of the deep well centred at R in the potential (2).

Accurate ab-initio computations [46–49] confirmed the results [45] of approximate calculations based on density functional theory that the crystalline environment hardly affects either the charge distributions or the polarizabilities of cations having s^2 or p^6 outermost electronic configurations. This insensitivity of such cations to their environment suggests that it will be adequate to use the following very simple approximation [4] to the function $F^{(0)}_{env}(r_C;R)$ in which this is constant from $r_C = 0$ to $r_C = R$ after which it decreases:

$$F^{(0)}_{env}(r_C;R) = \phi_{envC}/R \qquad r_C \leqslant R \tag{21a}$$

$$F^{(0)}_{env}(r_C;R) = \phi_{envC}/r_C \qquad r_C \geqslant R \tag{21b}$$

Here the constant ϕ_{envC} is chosen to make the potential (21a) reproduce that due to the point charge lattice for distances r_C less than R. Hence the form (21) for $F^{(0)}_{env}(r_C;R)$ is correct for distances r_C which are sufficiently small that the electron density originating from neighbouring ions is negligible because for such distances the true potential (3) does not deviate from that (1) generated by a point charge lattice. The approximate calculations of Mahan [45] suggest that the hump present in the full potential (3) at larger values of r_C but absent from that generated by the point charge

lattice (1) is quite small (see Figure 3 of [45]). In view of the insensitivity of cation electrons to their environment, at least for ions having s^2 or p^2 outermost electronic configurations, it is not unreasonable to neglect this hump entirely. The model (21) for the spherically symmetric part $F_{env}^{(0)}(r_C;R)$ of the environmental potential acting on a cation electron has therefore been used in all the calculations to be presented here unless explicitly stated to the contrary. Since the electron density of cations is negligible in regions of space where r_C is greater than R, the potential (21) effectively reduces to a constant which would not therefore affect the orbital wavefunctions. Consequently it is not surprising that cation electron density distributions computed using the form (21) for $F_{env}^{(0)}(r_C;R)$ are virtually unchanged from those of the free cations [4].

2.4 The Watson Shell Model For The Environmental Potential

An old method for approximating the environmental potential is that introduced by Watson [53] to describe the O^{--} ion in an ionic solid. In this model the environmental potential $F_{env}(\mathbf{r}_X;R)$ for an electron belonging to ion X is taken to equal the potential generated by a spherical shell which has a radius equal to the ionic radius (R_{OX}) of ion X and carries a charge equal in magnitude but opposite in sign to that (q_X) of ion X [53–55]. Thus

$$F_{env}(\mathbf{r}_X;R) = q_X/R_{OX} \qquad r_X \leqslant R_{OX} \tag{22a}$$

$$F_{env}(\mathbf{r}_X;R) = q_X/r_X \qquad r_X \geqslant R_{OX} \tag{22b}$$

For anions in crystals near their equilibrium geometries the behaviour of the Watson potential (22) is qualitatively similar to the model (19) because the potential inside a spherical shell of positive charge is both constant and stabilizing for an electron whilst (22) behaves as r_A^{-1} outside the shell. Furthermore since the quantity $R - R_0$ will be equal to the cation radius for the one geometry $R = R_e$, the increases of both the Watson potential and that (19) from their constant values at small r_A will start at the same value of r_A. It has been further found [4] that for $R = R_e$ the constant $k_{env,A}$ is approximately equal to the magnitude of the anion charge. This causes the environmental potential generated by the Watson model to be very similar to that (19) for this one value (R_e) of R. However this is not the case for R values differing significantly from R_e because the length of the constant region (19a) of the potential (19) increases with R whilst its depth decreases unlike that in the Watson model where this constant region of the potential remains unchanged as R is varied. Thus the potential (19) vanishes as R tends to infinity whereas this is not the case for the Watson model (22). The predictions generated using (19) are compared with those derived using the physically less realistic Watson model in section 2.5.

The environmental potential (22) was introduced for cations [54,55] on the grounds that it was the application to these systems of the ideas of Watson [53]. For cations in crystals having the NaCl structure as well as those having the fluorite structure, the environmental potential (22) generated by this Watson model is compared in Figure 5 with the model potential (21) [4] described in the last subsection. Both potentials have the same mathematical structure because both are initially constant from $r_C = 0$ and decrease as r_C^{-1} at larger distances. However the Watson model is very different physically from (21) since the cation radius is so much less than R that cation orbitals have appreciable magnitudes in the regions of space for which r_C is greater than the

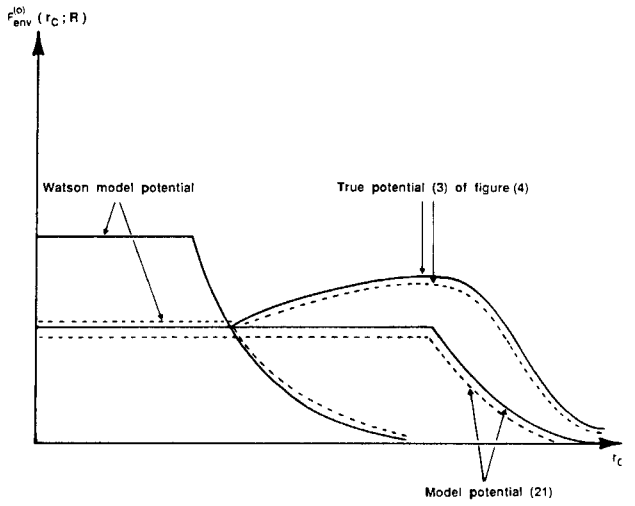

Figure 5 Comparison of different models for the spherically symmetric part of the environmental potential acting on a cation electron. (solid curves denote fluorite structure and dotted curves the NaCl structure).

cation radius. This causes the orbitals computed using this Watson potential to be expanded relative to those of the free cation since the electron density will naturally be enhanced, at least slightly, in regions of space where the environmental potential is less repulsive than its constant value between zero and the cation radius. In contrast cation orbitals computed using the environmental potential (21) show no such expansions because the amplitudes of the orbitals have become negligible for values of r_C much less than the value R at which $F^{(0)}_{env}(r_C;R)$ ceases to be constant and begins to decrease. No justification for the extension [54,55] of the Watson model to cations has ever been given. Furthermore since the resulting potential is qualitatively quite unlike the more realistic potential (3) of Figure 4, it must be concluded that it is incorrect to apply the Watson potential to cations and hence that the orbital expansions predicted with its use are spurious. For the fluorite structure these spurious expansions originating from the incorrect decrease of $F^{(0)}_{env}(r_C;R)$ for r_C greater than the cation radius are enhanced because the constant potential provided by the Watson model for smaller values of r_C is too large. Thus for the Pb^{++} ion in the cubic form of PbF_2 the Watson model yields a constant potential equal to 0.87 a.u. whereas the correct value provided by (21) is only 0.67 a.u. at $R = R_e$. These errors cause the 6s orbital computed using this Watson model to be too expanded having a mean radius of 2.60 a.u. compared with one of 2.23 a.u. calculated using the environmental potential (21). The orbitals of the Pb^{++} ion generated by the latter computation are almost unchanged from those of the free Pb^{++} ion.

Here it is appropriate to note that the polarizabilities computed for cations in ionic crystals by Schmidt *et al.* [55] are unreliable because the Watson potential was used to simulate the effects of the environment on the cation electrons. The polarizabilities they predict [55] for free cations, where no environmental potential was used, are very reasonable agreeing to within 10% with the best values [44] currently available which are presented in Table 9. However their predictions [55] for the polarizabilities of

cations in crystals are too large because the Watson potential was used to simulate the effects of the crystalline environment. For the larger and more polarizable cations in crystals, their predictions are usually too large by about 50%.

It is interesting to extend the study, described in section 2.2(ii), of the cohesion of the NaF crystal at R = 4.5 a.u. to include the Watson model description (22) of both the cation and anion environments. For the F^- ion, the rearrangement energy of 10 kJ $mole^{-1}$ and $2p$ orbital mean radius of 1.22 a.u. are essentially unchanged from those predicted using the model (19) for the environmental potential. This shows that the F^- ion wavefunctions generated by the two models are virtually identical. For the reasons discussed in section 2.2 this is not unexpected for an anion in a crystal having an R value close to R_e. However use of the Watson model generates a wavefunction for the Na^- ion that is slightly but significantly expanded compared with that of the free ion, the $2p$ orbital having a mean radius of 0.801 a.u. compared with one of 0.797 a.u.. This expansion is sufficiently small that the computed short range repulsion $V^0_{sNa^+F^-}(R)$ remains unchanged from that reported in the last column of Table 4 whilst 4 kJ $mole^{-1}$ of energy have been lost in making even this slight rearrangement of the electronic structure of the Na^+ ion. Consequently the total rearrangement energy of 14 kJ $mole^{-1}$ is larger that of 10 kJ $mole^{-1}$ reported in the last column of Table 4. This causes the crystal cohesion of 904 kJ $mole^{-1}$ predicted using the Watson model for both the Na^+ and F^- ions to be marginally less than that obtained (column 4 of Table 4) using free Na^+ wavefunctions. In contrast to that generated using the Watson shell model, the wavefunction for the Na^+ ion computed using the physically realistic model (21) for the environmental potential acting on an Na^+ electron is essentially identical to that of the free Na^+ ion. This further illustrates the failure of the Watson shell model for cations. It can therefore be concluded from the calculations reported in Table 4 that the use of the environmental potential (19) for anions and that (21) for cations is to be greatly preferred over any of the other methods so far considered.

2.5 *Comparison Of Wavefunction Adaption Methods*

In this section the different methods which have been used to adapt the ion wavefunctions to the crystalline environment are further tested by comparing the predicted crystal properties with experiment. The function $U_L(R)$ for the crystal cohesion was computed using the most accurate expression that is currently available without considering 3-body terms, namely that (14). This procedure thereby includes both the short range correlation potentials $V^{corr}_{sXY}(x_{XY}R)$ as well as the dispersion energy $U_{disp}(R)$ calculated as described section 3 with the inclusion of the damping of the dispersive attractions within the closest cation–anion, cation–cation and anion–anion pairs. The short range correlation terms were computed from the approximation provided by density functional theory originally used by Gordon and Kim [8]. The uncorrelated short range interactions $V^0_{sCA}(R)$ within the closest cation–anion pairs were computed using the RIP programme which yields results which are exact once the wavefunctions for the two ions have been specified. The results reported in the first three numerical columns of Table 5 were derived with the uncorrelated short range interactions $V^0_{sCC}(x_{CC}R)$ and $V^0_{sAA}(x_{AA}R)$ computed using the Lloyd and Pugh [56] variant of density functional theory. As discussed in section 4, density functional theory gives rise to several variants of which that due to Lloyd and Pugh is one of the two more reliable. Since the results reported in these three columns were obtained using the accurate expression (14) and differ solely in the method used to adapt the wavefunc-

Table 5 Comparison of different methods for adapting ions wavefunctions to the crystalline environment[1,2,3]

		Model environmental potential				
		free	*Watson*	*model (19) + (21)*	*model*[4] *(19) + (21)*	*expt*[5]
LiF	D_e	957	1006	1007	1038	1036
	R_e	4.19	4.02	3.99	3.885	3.806
	B	5.08	8.63	7.05	8.16	6.98, 7.2, 8.67
AgF	D_e	930	940	934	944	942, 953
	R_e	4.73	4.65	4.70	4.642	4.658
	B	6.29	7.46	6.40	6.37	
PbF_2	D_e	2330	2385	2406	2433	2491
	R_e	5.05	4.77	4.90	4.866	4.861
	B	5.37	9.39	6.26	6.56	6.53

[1] All results from [4] and computed from expression (14) for $U_L(R)$ thus including both the short range correlation term $V_{sXY}^{corr}(x_{XY}R)$ and the damped dispersion energy $U_{disp}(R)$.
[2] $V_{sCA}^0(R)$ computed using the RIP programme but $V_{sCC}^0(x_{CC}R)$ and $V_{sAA}^0(x_{AA}R)$ calculated from the Lloyd and Pugh [56] variant of density functional theory except for the last column where these latter two potentials were also computed using the RIP programme.
[3] Lattice energies D_e in kJ mole^{-1}, closest equilibrium cation–anion separations R_e in a.u. and bulk compressibilities B in 10^{12} Nm^{-2}.
[4] Method of calculations differs from that in previous column as explained in note (2).
[5] See [4] and [5] for sources of experimental results.

tions to the crystalline environment, their comparison provides a useful test of the different descriptions of the environmental potential. The results presented in the fourth column differ from those of the third only in that the two short range interactions $V_{sCC}^0(x_{CC}R)$ and $V_{sAA}^0(x_{AA}R)$ were computed using the RIP programme rather than density functional theory.

There are five main conclusions to be drawn from the results assembled in Table 5. Firstly the use of free ion wavefunctions predicts insufficiently strong binding as manifested by calculated lattice energies and compressibilities that are too small and calculated R_e values that are too large (column 1). This shows that the environmentally induced modifications of the ion wavefunctions cannot be ignored if the crystal properties are to be described accurately.

Secondly the calculations (column 2) using the Watson shell model to describe the environmental potentials agree better with experiment than those derived using free ion wavefunctions. The anion wavefunctions used in the Watson model calculations will be quite accurate for R values in the vicinity of R_e because these functions are similar to those derived using the more accurate representation (19) of the environmental potential. The wavefunctions computed for the light cations Li^+ and Na^+ are very little affected by the Watson shell potential even though this is qualitatively incorrect. Hence for LiF the results (column 2) predicted through its use are very similar to those column (3) derived using the more accurate environmental potentials (19) and (21). This is also the case for NaF and NaCl, the results for these systems being presented in Table 5 of [4].

The third conclusion to be drawn from Table 5 is that the predictions obtained for PbF_2 using the Watson shell model are not entirely satisfactory because these underestimate the lattice energy D_e whilst predicting too high a bulk compressibility with

too small an equilibrium closest cation–anion separation R_e. This is an undesirable combination of errors. This calculation fails because use of the Watson shell potential generates a Pb^{++} wavefunction which is far too expanded thus predicting a Pb^{++} rearrangement energy as large as 187 kJ mole $^{-1}$. Use of the more realistic model (21) for the environmental potential yields a Pb^{++} rearrangement energy of only 0.5 kJ mole^{-1} for R values close to R_e. The excessive expansion of the Pb^{++} ion generated using the Watson model potential originates from the physically incorrect form of this potential that is shown in Figure 5.

The fourth conclusion to be drawn from Table 5 is that the results (column 3) computed using the environmental potential (21) for the cations and (19) for the anions are in much better agreement with experiment than those computed using either free ion wavefunctions (column 1) or the Watson shell potential (column 2). In particular the unsatisfactory features of the predictions for PbF_2 (column 2) are eliminated when the physically realistic environmental potentials (19) and (21) are used in place of the Watson shell potential. Figure 6 illustrates the qualitative differences between the cohesive energy curves $U_L(R)$ generated using these three methods. For R values in the vicinity of R_e the use of the environmental potentials (19) and (21) yields the most negative values of $U_L(R)$ whilst the use of free ion wavefunctions produces the least negative ones (curve 1 in Figure 6). For these R values, the energies $U_L(R)$ (curve 2 in Figure 6) computed using the Watson shell potential lie between the free ion ones and those derived using (19) and (21) although they are significantly closer to the latter. As R tends to infinity the environmental potentials (19) and (21) tend to zero so that the ion wavefunctions computed pass smoothly over into those of the free ions. Consequently, for large R values the $U_L(R)$ curve predicted using (19) and (21) approaches that computed using free ion wavefunctions. In the

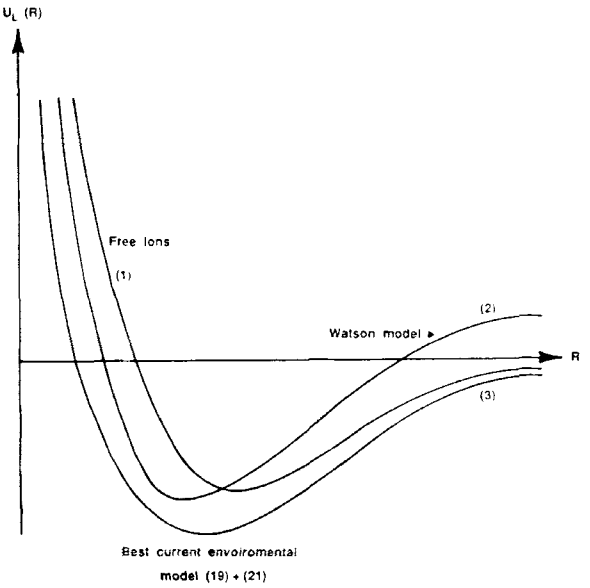

Figure 6 Comparison of crystal cohesive energy functions $U_L(R)$ predicted using different models for the crystalline environment.

limit that R tends to infinity all the inter-ionic potentials $V_{sXY}^{T}(x_{XY}R)$ vanish so $U_L(R)$ also tends to zero for both the free ion model (curve 1 of Figure 6) as well the curve 3 generated using (19) and (21). This is however not the case for the $U_L(R)$ curve calculated using the Watson shell potential because neither the radius of this shell being taken as the ionic radius nor the charge carried by the shell change with R. Consequently the same ion wavefunctions are used for all values of R thereby causing $U_L(R)$ to tend to the total rearrangement energy rather than to the correct value of zero. If this overestimation of $U_L(R)$ at large R is very pronounced, as is the case for PbF_2, then the entire curve will be skewed. For PbF_2 this explains both why the bulk compressibility is so greatly overestimated and why R_e is underestimated even though the predicted D_e is less than that derived using the environmental potentials (19) and (21). For systems such as LiF where the incorrect behaviour at large R is less pronounced because the rearrangement energy derived from the Watson model is less, the skewing of the curve in the vicinity of R_e is sufficiently small that the shortcomings of this model are not noticable.

It can be concluded both by comparing with experiment the results in the first three columns of Table 5 as well as by examining Figure 6 that the use of the environmental potentials (19) and (21) is to be greatly preferred either to invoking the Watson shell model or to neglecting altogether the effects of the crystalline environment. In particular the environmental potentials (19) and (21) do not suffer from any of the defects of the other potentials considered. Although one should expect further research to produce more accurate representations of the environmental potentials, one should not expect these to show any major qualitative differences from those (19) and (21) because these correctly model the dominant features of the 'true' environmental potential.

The fifth main conclusion to be drawn from the results assembled in Table 5 is that one should avoid using density functional theory to compute the uncorrelated short range potentials even within pairs of ions such as the closest cation–cation and anion–anion ones which are not those having the smallest inter-ionic separation (R). Thus the results reported in column 4 derived using the RIP programme to compute all three uncorrelated short range potentials $V_{sCA}^{0}(R)$, $V_{sCC}^{0}(x_{CC}R)$ and $V_{sAA}^{0}(x_{AA}R)$ agree significantly better with experiment than do those (column 3) in which the latter two uncorrelated short range potentials were computed using the Lloyd and Pugh [56] version of density functional theory. However the errors introduced by using density functional theory for the latter two inter-ionic potentials are not so major as to invalidate the conclusions concerning the merits of the different environmental potentials which were drawn from the results presented in the first three columns of Table 5.

2.6 Summary

Anions are significantly affected by the crystalline environment which contracts their charge distributions and reduces their polarizabilities when compared with the free ions. The reduction of the uncorrelated short range repulsion between an anion and its closest cation neighbours that accompanies the contraction of its charge density is appreciable and therefore cannot be neglected in calculations aiming for high accuracy. The model potential (19) for representing the spherically symmetric part of the environment potential acting on anion electrons contains the qualitative features of the true potential. This model would seem to be the best currently available for

calculating anion wavefunctions adapted to the crystalline environment which wavefunctions can then be used as input to a programme such as RIP to compute the inter-ionic potentials. Other possible models for the environmental potential are reviewed elsewhere [5].

Cations having s^2 or p^6 outermost electronic configurations are essentially unaffected by their environment in the crystal and thus have the same charge distributions and polarizabilities as those of the free ions. The Watson shell model potential (22) for representing the influence of the environment on cation electrons is qualitatively incorrect and its use can yield cation wavefunctions that are spuriously expanded compared with those of the free ion. This objection does not apply to the model (21) of the spherically symmetric part of the environmental potential for cation electrons.

3. DAMPING OF RELIABLY CALCULATED INTER-IONIC DISPERSIVE ATTRACTIONS

3.1 Theory Of The Dispersive Attractions

3.1(i) The dispersive attraction within a single pair of ions

It is helpful to begin the study of the dispersive attractions in ionic crystals by considering the interaction of just two ions to be designated *a* and *b*. The simplest wavefunction for this pair is constructed as the product of the ground state wavefunction of ion *a* with that of ion *b*, which product is anti-symmetrized in order to take account of the Pauli principle. Such a wavefunction is not an exact eigenfunction of the full Hamiltonian operator for this pair because this operator contains terms, to be called the interaction Hamiltonian, which are illustrated in Figure 7. The interaction Hamiltonian is the sum of the terms which describe the attraction of the electrons on ion *a* to the nucleus of ion *b*, the attraction of the electrons on ion *b* to the nucleus of ion *a*, and the repulsion between the electrons on ion *a* with those on ion *b*. The evaluation of the energy using the full Hamiltonian but the above simplest wavefunction corresponds to treating the interaction Hamiltonian to just first order in perturbation theory. After subtracting the energies $E_a(R)$ and $E_b(R)$ of the non-interacting species, this approximation yields the interaction energy $V^0_{ab}(x_{ab}R)$. It is the treatment [20] of the interaction Hamiltonian to second order in perturbation theory, using a second quantized formalism taking account of exchange of electrons between the ions, that yields the interaction energy ($V_{ab}(x_{ab}R)$) already presented in equation (12). The second ($V^{disp}_{ab}(x_{ab}R)$) of the two terms in (12) additional to $V^0_{ab}(x_{ab}R)$ constitutes the dispersive attraction between the two ions. Although this term does not involve the exchange of electrons between the ions and does not vanish in the limit that the overlap of the ion wavefunctions has become negligible, it is still valid even when such overlap is appreciable.

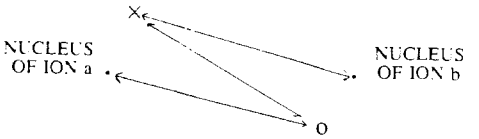

Figure 7 The electrostatic terms composing the interaction hamiltonian for the pair of ions *a* and *b*. (cross denotes an electron of ion *a* and the circle that of ion *b*)

The dispersive attraction $V_{ab}^{disp}(x_{ab}R)$ can be derived more conventionally [57] without recourse to a second quantized formalism by taking the unperturbed ground state to be just the simple product of the ground state wavefunctions of the two ions without introducing the anti-symmetrizer that takes account of the exchange of electrons between them. Starting from this assumption, the generation of the dispersive attraction by treating the interaction hamiltonian to second order in perturbation theory confirms that this attraction does not originate from processes involving any exchange of electrons between the two ions. As derived by both Kreek and Meath [57] and Boehm and Yaris [20] $V_{ab}^{disp}(x_{ab}R)$ does not take the familiar form of a series of terms the leading member of which is a dispersion coefficient divided by $(x_{ab}R)^6$. The form for the dispersion energy in (12) derived by Kreek and Meath is designated the non-expanded dispersion energy; the result derived by Boehm and Yaris is identical although it appears in a different mathematical form. The non-expanded dispersion energy is valid for all internuclear separations $x_{ab}R$ and does not diverge when $x_{ab}R$ tends to zero. Currently there seem to be two different methods for manipulating the non-expanded dispersion energy with the aim of converting it to a form which is both physically more transparent and of greater utility computationally. In the first of these, the theory is formulated in real space and the interaction Hamiltonian expanded into a multipole series. In the second approach, the theory is formulated in momentum space and the interaction Hamiltonian is expanded into a series of terms containing spherical harmonics and spherical Bessel functions.

It is the first of these procedures [57,58] in which the interaction Hamiltonian is expanded in the multipole series that yields the most familiar form for the dispersion energy where this is expressed as a series of terms involving inverse powers of $x_{ab}R$. This multipole expansion, which is only valid if the overlap between the ion wavefunctions is negligible, converts $V_{ab}^{disp}(x_{ab}R)$ into the form $V_{un\,ab}^{disp}(x_{ab}R)$ called the expanded dispersion energy [57]

$$V_{un\,ab}^{disp}(x_{ab}R) = -\sum_{n=6,8,\text{even}}^{\infty} C_n(ab)\,(x_{ab}R)^{-n} \tag{23}$$

Here $C_n(ab)$ is a dispersion coefficient which is independent of the distance $x_{ab}R$. The series (23) does not converge if all the infinite number of terms in it are summed. Although (23) is not a convergent series, it provides an asymptotic representation [59] in that the terms initially decrease with increasing n and then for larger n start to diverge. The optimal approximation is provided by summing all the terms up to the smallest one, including only one half of the latter [58]. The first term in (23) $-C_6(ab)(x_{ab}R)^{-6}$ is called the dipole–dipole dispersion energy because it originates from the interaction of an instantaneous dipole moment on one ion with the dipole induced on the other ion by the first instantaneous dipole. The second term $-C_8(ab)(x_{ab}R)^{-8}$ is designated the dipole-quadrupole dispersion energy since it arises from the interaction of the quadrupole moment on one ion induced by the instantaneous dipole on the other ion. Typically the dipole–dipole dispersion energy is significantly larger than the dipole–quadrupole dispersion energy, by a factor 3 to 4 for moderate values of $x_{ab}R$. It is not common to consider the terms in (23) having higher values for n partly because these are expected to be small and partly because knowledge of the corresponding dispersion coefficients is extremely limited. Thus, even for pairs of inert gas atoms, there are no reliable values for the $C_n(ab)$ coefficients having n greater than 10, whilst even the $C_{10}(ab)$ coefficients are not known for pairs of ions in crystals. The expanded form (23) for the dispersion energy is often called the undamped dispersion

energy, as indicated by the subcript 'un', in contrast to the damped dispersion energy that is derived by using the second of the two possible expansions of the interaction Hamiltonian which was discussed above.

Use of the undamped dispersion energy (23) for the closest pairs of ions is apriori inconsistent. Thus (23) is not valid if the overlap between the ion wavefunctions is not negligible. However for R values in the vicinity of R_e this overlap cannot be negligible because it is the origin of the short range repulsive forces which prevent an ionic crystal from collapsing under the coulombic attractions between the ions. An alternative expansion of the dispersion energy $V_{ab}^{disp}(x_{ab}R)$, valid for non-zero overlap of the ion wavefunctions, can be derived [6,7] by working in momentum space and then expanding the interaction hamilonian, not in the multipole series, but into a series of terms each containing spherical harmonics and spherical Bessel functions. This procedure, whose mathematical details need not be presented here, yields the damped dispersion energy

$$V_{ab}^{disp}(x_{ab}R) = -\sum_{n=6,8,\text{even}}^{\infty} \chi_n^{ab}(x_{ab}R)\ C_n(ab)(x_{ab}R)^{-n} \tag{24}$$

This result differs from the undamped dispersion energy (23) in that each term is multiplied by a dispersion damping function $\chi_n^{ab}(x_{ab}R)$. These functions are unity for distances $x_{ab}R$ which are sufficiently large that the overlap of the ion wavefunctions is negligible. However the $\chi_n^{ab}(x_{ab}R)$, although always positive, become less than unity for distances $x_{ab}R$ at which ion wavefunction overlap is appreciable. The dispersion damping functions thus reduce the magnitudes of the undamped energies $-C_n(ab)(x_{ab}R)^{-n}$ when this overlap is not negligible. For inter-ionic distances where this overlap is appreciable, the damping functions $\chi_n^{ab}(x_{ab}R)$ decrease rapidly with increasing n so that terms with high n in (24) are unimportant. At large $(x_{ab}R)$ where the dispersion damping functions approach unity, the $(x_{ab}R)^{-n}$ dependence ensures that terms with large n are unimportant. Thus, in contrast to the undamped dispersion energy (23), the damped dispersion series can be expected to be convergent rather than asymptotic with the sum of all the terms on the right hand side of (24) reproducing the value on the left hand side.

3.1(ii) The total dispersion energy of an ionic crystal

The total dispersion energy of an ionic crystal can be derived by slightly generalizing the approach just outlined for the interaction of a single pair of ions. The hamiltonian for all the electrons in the crystal is partitioned into a sum of purely intra-ionic terms plus a sum of inter-ionic interaction terms. The latter consists of the sum over all pairs of ions of the interaction hamiltonian described above for a single pair of ions. Treatment of the latter sum to second order in perturbation theory then shows that the total dispersion energy is composed of a term of the type (24) for each pair of ions in the crystal, augmented by three-body and higher order multi-body terms. In the limit that the overlap of the ion wavefunctions is negligible, the leading contribution to the 3-body energy reduces to the sum over all triples of ions of the Axilrod-Teller or triple dipole dispersion energy [60] for a single ion triple.

After neglecting all 3-body and higher order multi-body contributions to the total crystal dispersion energy, this reduces to that designated $U_{disp}(R)$ which consists of the sum of the interactions (24) for all pairs of ions

$$U_{disp}(R) = -\sum_{a=1}^{N_{ion}-1}\sum_{b=a+1}^{N_{ion}}\sum_{n=6,8,\text{even}}^{\infty}\chi_n^{ab}(x_{ab}R)\,C_n(ab)(x_{ab}R)^{-n} \quad (25)$$

Since the dispersion damping functions only deviate from unity when ion wavefunction overlap is non-negligible, all the dispersion damping functions in (25) can be replaced by unity excepting those for the closest cation–anion, cation–cation and anion–anion pairs. After making these replacements and retaining only the dipole–dipole and dipole–quadrupole terms, $U_{disp}(R)$ is given by

$$U_{disp}(R) = U_{disp}^{un}(R) + U_{disp}^{cd}(R) \quad (26)$$

Here $U_{disp}^{un}(R)$ is the undamped dispersion energy of the crystal predicted if all the dispersion damping functions are replaced by unity whilst $U_{disp}^{cd}(R)$ is the correction which replaces the undamped by the damped dispersion energy for those closest pairs of ions just mentioned. Hence this is given by

$$U_{disp}^{cd}(R) = -\sum_{n=6,8}\{n_{CA}(\chi_n^{CA}(R)-1)\,C_n(CA)\,R^{-n} + (1/2)$$
$$\times\,[n_{cc}(\chi_n^{CC}(x_{CC}R)-1)\,C_n(x_{CC}R)^{-n} + m\,n_{AA}(\chi_n^{AA}(x_{AA}R)-1)\,C_n(AA)(x_{AA}R)^{-n}]\} \quad (27)$$

In the undamped dispersion energy sum obtained by setting all dispersion damping functions to unity in (25), both the dipole–dipole and dipole–quadrupole terms have a known inverse sixth or inverse eighth power dependence on the distances $x_{ab}R$. Hence for given n the dispersive attraction between ion a of type X and ion b of type Y is related to attraction of the closest XY pair by multiplication by the factor $(x_{ab}/x_{XY})^{-n}$. Since this factor is purely geometrical, all the terms having the same n and pertaining to the same type (XY) of pair of ions in the expression yielding the undamped dispersion energy can be summed to yield a result proportional to R^{-n}. The undamped dispersion energy can therefore be expressed as

$$U_{disp}^{un}(R) = -\sum_{n=6,8}[S_n(CA)\,C_n(CA) + (1/2)\,(S_n(CC)\,C_n(CC) + m\,S_n(AA))]R^{-n} \quad (28)$$

Hence the constant $S_n(XY)$ is a purely geometrical factor which yields the undamped R^{-n} dispersion interaction of one ion of type X with all the other ions of type Y as $-S_n(XY)C_n(XY)R^{-n}$. Numerical values of these constants for some common crystal structures have been presented elsewhere [4,5], at least two sets of workers concurring with these values. Errors in some previous calculations of these coefficients have been pointed out [5].

The evaluation through (26) to (28) of the total crystal dispersion energy requires knowledge of the $C_6(XY)$ and $C_8(XY)$ dispersion coefficients and of the dispersion damping functions $\chi_6^{XY}(x_{XY}R)$ and $\chi_8^{XY}(x_{XY}R)$. The derivation of reliable values for the dispersion coefficients is discussed in section 3.3. The fundamental formalism developed by Jacobi and Csanak [6] has been used [4] to derive approximate forms for the dispersion damping functions which, being rather complicated, need not be presented here. Each of the damping functions $\chi_n^{XY}(x_{XY}R)$ depends on two dispersion damping parameters, one for each ion. As discussed more fully elsewhere [4,5], the

damping parameter for ion X can be calculated from the eigenvalues of the outermost orbital in the ground state and first relevant excited state of the ion. Here it is only necessary to point out that, although there is a loose correlation between these eigenvalues and the mean radii of the relevant orbitals, it appears to be undesirable to use this in the calculation of the dispersion damping parameters [4,5]. It is most likely that the results of Jacobi and Csanak [6] would have been improved had they derived these parameters from the eigenvalues and not the mean radii. Since the details of the calculation of the dispersion damping parameters and hence of the damped dispersion energy have been presented elsewhere [4,5] these need not be reported here. For this talk, it is only necessary to point out that the damped dispersion energy $U_{disp}(R)$ can now be calculated as had to be done in the ab-initio study [4] of the properties of ionic crystals.

3.2 The Influence Of Dispersion Damping On The Crystal Properties

The importance of the inter-ionic dispersive attractions and their damping originating from the overlap of the ion wavefunctions is illustrated by the results assembled in Table 6. Comparable results were found for all the crystals examined in the study [4]. In all these calculations the crystal cohesion $U_L(R)$ was evaluated from an expression which differs from (14) solely in the treatment of the contribution arising from the inter-ionic dispersive attractions. Thus in all these calculations all three uncorrelated short range interactions $V^0_{sCA}(R)$, $V^0_{sCC}(x_{CC}R)$ and $V^0_{sAA}(x_{AA}R)$ were computed with the RIP programme using as input ion wavefunctions which had been adapted to the crystalline environment using the best of the models described in section 2, namely that based on equations (19) and (21). Since furthermore the short range correlation terms $V^{corr}_{sXY}(x_{XY}R)$ were also included in all three sets of calculations, these differ only in the computation of the contributions originating from dispersion. This contribution was computed using the dispersion coefficients, damping functions and dispersion damping parameters derived previously [4].

There are three main conclusions to be drawn from the results presented in Table 6. The first of these is drawn by comparing with experiment the results presented in the first numerical column which were derived by omitting altogether the dispersion contribution $U_{disp}(R)$ to the crystal cohesion. This comparison shows that insufficient cohesion is predicted with the omission of $U_{disp}(R)$, as manifested by predicted lattice energies and compressibilities that are too small, and equilibrium closest cation–anion separations that are too large. This shows that the dispersion plays a significant role in the cohesion of crystals such as AgF and PbF_2 for which the $C_6(XY)$ dispersion coefficients are appreciable on account of the high polarizability of the ions.

The second conclusion is drawn by comparing with experiment the results assembled in the second numerical column which were derived by replacing $U_{disp}(R)$ in (14) by $U^{un}_{disp}(R)$ (28) thereby omitting the damping of the dispersion which arises when the overlaps of the wavefunctions of the interacting ions are not negligible. The significant overestimation of the crystal cohesion as manifested by too large predicted lattice energies and compressibilities and too small predicted R_e values shows the damping of the dispersive attractions is appreciable and cannot be neglected. This overestimation of the cohesion is especially marked for AgF where the dispersion accounts for some 7% of the total lattice energy.

The results presented in the third numerical column of Table 6 were derived from (14) and thus include not only the dispersive attractions but also their damping

Table 6 The influence of dispersion and dispersion damping on crystal properties[1,2]

		dispersion neglected	*undamped dispersion*[4]	*damped dispersion*[5]	*expt*[3]
AgF	D_e	881	1086	944	942, 953
	R_e	4.77	4.19	4.642	4.658
	B	5.21	10.99	6.37	
PbF_2	D_e	2336	2530	2433	2491
	R_e	4.99	4.64	4.866	4.861
	B	5.62	7.44	6.56	6.53

[1] All results from [4] calculated from an expression differing from (14) for $U_L(R)$ solely in the treatment of the dispersion energy. Thus all calculations include the short range correlation terms $V_{sXY}^{corr}(x_{XY}R)$ and all three uncorrelated short range interactions $V_{sCA}^0(R)$, $V_{sCC}^0(x_{CC}R)$ and $V_{sAA}^0(x_{AA}R)$ computed with the RIP programme using the model environmental potentials (19) and (21).

[2] Lattice energies D_e in kJ mole^{-1}, closest equilibrium cation–anion separations R_e in a.u. and bulk compressibilities B in 10^{12} Nm^{-2}.

[3] See [4] and [5] for sources of experimental results.

[4] $U_L(R)$ calculated by replacing the damped dispersion in (14) by the undamped dispersion energy $U_{disp}^{un}(R)$ (28).

[5] $U_L(R)$ calculated from (14) with damped dispersion energy $U_{disp}(R)$ evaluated from (26).

originating from the overlaps of the ion wavefunctions. The third conclusion to be drawn from Table 6 is that this damping is very significant and that it cannot be ignored in calculations aiming to achieve any reasonable degree of accuracy. Thus its incorporation eliminates the overestimation of the cohesion predicted (column 2 of Table 6) when the dispersion is introduced in its undamped form. Furthermore the results of the calculations including the damped dispersion are in very good agreement with experiment. A detailed analysis of the results shows that, for the closest-anion pairs in crystals having geometries close to equilibrium, the damping roughly halves the dipole–dipole dispersion energy whilst reducing the dipole–quadrupole energy by a factor of between three and four [4]. For the closest cation–cation and anion–anion pairs both the dipole–dipole and dipole–quadrupole energies are reduced to about 80% of their undamped values at these crystal geometries.

3.3 The Derivation Of Reliable Values For The Dispersion Coefficients

3.3(i) Overview

The results presented in Table 6 show that the dispersive attractions between the ions are sufficiently important that it is necessary to use accurate values for the dispersion coefficients $C_6(XY)$ and $C_8(XY)$ in high precision calculations of crystal properties. It is especially important to use accurate values for the $C_6(XY)$ coefficients because the dipole–dipole dispersion energy makes the largest contribution to $U_{disp}(R)$, this being typically three to four times greater than the dipole–quadrupole term for crystals near their equilibrium geometries. Although it may seem to be a truism to say that one should use accurate values for the dispersion coefficients, a very large fraction of the literature concerning their numerical values for ions in crystals is unreliable. Thus, for a not inconsiderable number of such coefficients, one can find literature values differing by factors of up to six whilst for $C_6(F^- F^-)$ values differing by a factor as large as 50 have been reported. For the $C_6(XY)$ coefficients it is only surprisingly recently that these discrepancies have been resolved [49] and reliable values reported for them for ions in crystals. There is still a need for further progress in the determination of $C_8(XY)$ coefficients for ions in crystals although recent work has not only generated a number of accurate values for ions of low nuclear charge [50] but also provided values in error by no more than 25% for a much wider range of systems [4,50]. It has also been demonstrated [4,59] that a number of other approximate methods are untrustworthy because they generate results in error by several hundreds of percent.

There are, in principle, three distinct approaches for deriving values of $C_n(XY)$ dispersion coefficients. In the first of these, the coefficients are deduced, using exact quantum mechanical formulae, from experimentally measured values of either the oscillator strength function or refractive indices [61,62]. However although this approach has provided reliable values of $C_n(XY)$ coeffients for species in the gas phase, its application to ions in solids encounters problems, reviewed elsewhere [5], that render its predictions untrustworthy. The second approach for deriving values of $C_n(XY)$ coefficients is to compute these *ab-initio* using the methods of non-relativistic quantum chemistry. Special techniques [46] have to be used to describe the influence of the crystalline environment on the pair of ions X and Y for which the $C_n(XY)$ coefficient is to be computed. Although this is a most promising approach, at least for ions of not too high atomic numbers, it has so far been applied only at the Coupled Hartree–Fock level which does not take full account of electron correlation. Never-

theless it has provided the most accurate values currently available for $C_8(XY)$ coefficients for ions in crystals [50]. Although such computations have provided valuable insights in the mechanisms through which $C_6(XY)$ coefficients are influenced by the crystalline environment [49], the incomplete treatment of electron correlation has prevented them from yielding numerical values more accurate than those provided by the third approach. The third approach for determining $C_n(XY)$ coefficients is either to use a semi-empirical formula such as that due to Slater and Kirkwood [63] or to envoke a simple non-empirical approximation such as that due to Starkschall and Gordon [64]. The latter expresses the $C_n(XY)$ coefficients having n greater than 6 in terms of the $C_6(XY)$ coefficient and the expectation values of various powers of the electron nuclear distances taken over just the ground state wavefunctions of the interacting species. Even though the Starkschall Gordon formula usually underestimates $C_8(XY)$ dispersion coefficients by some 10% to 20%, it had to be used [4] for those systems containing heavy ions for which *ab-initio* quantum chemistry computations are not feasible. Here the derivation of $C_8(XY)$ dispersion coefficients will not be considered further partly because these are less important than the $C_6(XY)$ coefficients and partly because knowledge of methods for their derivation as well as of their numerical values is still in the process of evolution. Our current state of knowledge of these matters is reviewed in [5].

3.3(ii) Derivation of $C_6(XY)$ dispersion coefficients from the Slater-Kirkwood formula

Currently it is judicious application of the Slater-Kirkwood formula that yields the most accurate values for $C_6(XY)$ dispersion coefficients for ions in crystals. The reliability of a wide range of semi-empirical methods for determining $C_6(XY)$ dispersion coefficients was tested [4] by comparing their predictions for gas phase species against values accurately known either by derivation from experimental data [61,62] or from accurate *ab-initio* quantum chemistry calculations. These tests revealed that all the methods examined were unreliable with the exception of the Slater-Kirkwood formula. This relates $C_6(XY)$ to the static polarizabilities α_X and α_Y and electron numbers P_X and P_Y of the interacting species [63]. Thus

$$C_6(XY) = (3/2)\,\alpha_X\alpha_Y/[(\alpha_X/P_X)^{1/2} + (\alpha_Y/P_Y)^{1/2}] \tag{29a}$$

i.e.

$$C_6(XX) = (3/4)\,\alpha_X^{3/2}\,P_X^{1/2} \tag{29b}$$

The more recent derivation [65] of the Slater-Kirkwood formula considerably generalizes the original derivation thereby justifying the use of the most accurate values currently available for the polarizabilities. Both this generalization as well as the relation of the Slater-Kirkwood formula to other approximate results have been reviewed elsewhere [5].

The Slater-Kirkwood formula provides a rigorous upper bound to $C_6(XY)$ if the electron numbers P_X and P_Y are taken to equal the total numbers of electrons on the species X and Y respectively [65]. However, for all but the lightest systems, this upper bound does not provide a useful estimate of $C_6(XY)$ because the dominant contributions to the dipole–dipole dispersion energy come from only the most loosely bound electrons. Thus, for example, C_6(HgHg) is predicted [49] to be 1330 a.u. if P_{Hg} is taken to be 80 whilst the experimental value of C_6(HgHg) is only 240 a.u. [66]. An investiga-

Table 7 Electron numbers derived from species indicated and used for iso-electronic ions[1,2]

Species	*He*	*Ne*	*Ar*	*Kr*	*Xe*	*Ag^+*	*Hg*
Electron number	*1.430*	*4.455*	*6.106*	*7.305*	*7.901*	*5.863*	*2.605*

[1] Taken from [4] and derived from Slater-Kirkwood formula (29b).
[2] For all the neutral species polarizabilities and $C_6(XX)$ coefficients were derived from either experiment or accurate ab-initio quantum chemistry calculations taking account of electron correlation. For Ag^+ these two quantities were taken from the density functional calculations [67] for an isolated ion.

tion [4,49] of the best way of choosing the electron number showed that this should be taken to be the value which reproduces in (29b) the exact $C_6(XX)$ coefficient of the isoelectronic rare gas from the exact polarizability of that gas. The resulting electron numbers are assembled in Table 7. For the Tl^+ and Pb^{++} ions, the electron number is derived from the polarizability and $C_6(XX)$ coefficient for Hg [66]. To derive the electron number for Ag^+, one has to use the polarizability and $C_6(XX)$ coefficient computed [67] using density functional theory because there are no reliable data for any isoelectronic system.

Reliable predictions of the $C_6(XY)$ coefficients from the Slater-Kirkwood formula require accurate values for the static polarizabilities. It should be pointed out that for most ions there is a surprisingly wide range of values reported for the polarizabilities. Recent work [44,46–49] has not only shown why a very significant fraction of the earlier literature is unreliable but also presented accurate and trustworthy values for the static polarizabilities of a wide range of ions. These polarizabilities were obtained by combining experimental refractive index data with the results of *ab-initio* quantum chemistry computations. For a crystal, the total molar polarizability, denoted α_{cr}, can be derived using the Clausius-Mosotti relationship from the crystal refractive index extrapolated to infinite wavelength. The molar polarizability thus derived is then written as a sum of cation α_C and anion α_A contributions.

$$\alpha_{cr} = \alpha_C + m\,\alpha_A \tag{30}$$

Significant errors can be introduced if α_{cr} is derived from refractive index data which has not been extrapolated to infinite wavelength [44]. The polarizabilities of the small cations Li^+, Na^+, K^+, Mg^{++} and Ca^{++} are not only accurately known from ab-initio calculations taking account of electron correlation but are also independent of the particular crystal in which they are embedded [46,47]. The polarizabilities of anions in salts with these five cations can then be determined from the experimental values of α_{cr} by applying (30). In contrast to the cations, the anion polarizabilities are found to depend on the crystal. For halides, the values of α_A deduced through (30) are found to depend solely upon the closest cation–anion separation R and to be independent of the crystal type. For example, the fluoride ion polarizability in MgF_2 is the same as that in LiF because both these crystals have the same value of R even though the structures of these two crystals are naturally different. For halide ions the dependence of α_A on R can be represented as

$$\mathrm{Log}_{10}\alpha_A = A + B\,R^{-2} + C\,R^{-4} \tag{31}$$

The polarizabilities of both the O^{--} and S^{--} ions in their salts with the above five small cations have also been deduced from the experimental values of α_{cr} by applying (30). In contrast to halide ions, the polarizabilities of both O^{--} and S^{--} are found

to depend on the crystal structure as well as on R. For oxides and sulphides having the NaCl crystal structure, the anion polarizabilities can again be represented by a relation of the type (31) but with C set to zero. The numerical values of the constants A, B and C for both halide ions and O^{--} and S^{--} ions are assembled in Table 8. This data taken in conjuction with (31) enables one to predict the polarizabilities of these six anions in salts formed with cations other than Li^+, Na^+, Mg^{++} and Ca^{++}. Hence the polarizabilities of these other cations can be found through (30) from the experimental values of α_{cr}. The consistency of the cation values obtained [44] from salts formed with different anions not only confirms the validity of this procedure but also shows that the polarizabilities of cations having s^2 or p^6 outermost electronic configurations are independent of the crystalline environment. The correctness of this method was also corroborated by the agreement between the Rb^+ polarizability thus deduced [44] with that subsequently predicted [49] from *ab-initio* calculations including electron correlation. The polarizabilities of the heavier alkali and alkaline earth cations as well as those of Ag^+, Tl^+ and Pb^{++} deduced from experimental α_{cr} values are presented in Table 9 along with those of the five light cations. In contrast to the polarizabilities of cations having s^2 or p^6 outermost electronic configurations, the polarizability of 11.8 a.u. for Ag^+ in AgF differs significantly from that (9.2 a.u. [44]) of the free Ag^+ ion. For Ag^+ the deduction of an in-crystal polarizability different from that predicted by the free ion calculations [67] used to derive the electron number in Table 7 is entirely consistent with the approach of determining the electron numbers from data for an iso-electronic system. The physical origins of this environmentally induced enhancement of the Ag^+ polarizability have been discussed elsewhere [44].

Table 8 The constants A, B and C yielding the dependence of anion polarizabilities on the closest cation-anion separation[1,2]

Anion	F^-	Cl^-	Br^-	I^-	O^{--}	S^{--}
A	1.201	1.473	1.562	1.916	1.706	1.780
B	−9.204	−3.370	−1.582	−15.71	−10.31	−6.946
C	44.30	−23.47	−53.40	176.2	0.0	0.0

[1] Anion polarizabilities given by (31) given cation–anion separation R and the above constants A, B and C taken from [44]. All quantities in a.u.
[2] For halide ions the constants are independent of the crystal structure. Those for the oxide and sulphide ions only apply to crystals having the NaCl structure.

Table 9 Static polarizibilities of cations (a.u.)[1]

Ion (X)	α_X	*Ion (X)*	α_X	*Ion (X)*	α_X
Li^+	0.192	Be^{++}	0.052	Tl^+	28
Na^+	1.002	Mg^{++}	0.486	Pb^{++}	17.9
K^+	5.339	Ca^{++}	3.193	Ag^+ in AgF	11.825
Rb^+	9.05	Sr^{++}	5.20		
Cs^+	15.28	Ba^{++}	10.1		

[1] From accurate non-relativistic quantum chemistry computations including the effects of electron correlation for Li^+, Na^+, K^+ [47], Mg^{++} and Ca^{++} [48]. From such computations [49] and experimental refractive index data after subtracting anion polarizabilities derived from equation (31) for Rb^+. From experimental refractive index data after subtracting anion polarizability predicted by (31) for Cs^+, Sr^{++}, Ba^{++}, Ag^+, Tl^+ and Pb^{++} [44]. From coupled Hartree-Fock theory [91] (neglects electron correlation) for Be^{++}

The most reliable values currently available for the $C_6(XY)$ coefficients for ions in crystals are deduced [49] from the Slater-Kirkwood formula using the electron numbers reported in Table 7 and the cation polarizabilities presented in Table 9. For salts containing the cations listed in this Table the anion polarizabilities are derived through (30) by subtracting the cation polarizabilities from the experimental values of α_{cr}, whilst for salts with other cations the values of α_A are deduced from (31) and the cation polarizabilities then derived from (30). The $C_6(XY)$ coefficients derived by this method are slightly but significantly more reliable than those predicted from *ab-initio* quantum chemistry calculations at the Coupled Hartree-Fock level because the contributions to the $C_6(XY)$ coefficients arising from electron correlation are larger than the errors introduced by using the Slater-Kirkwood formula with the electron numbers of Table 7. For pairs of light ions it is now technically possible to refine the non-relativistic *ab-initio* computations to take account of electron correlation. However, for large anions such as Br^- and I^- in crystals containing cations as heavy as lead, such computations are not feasible even at the Coupled Hartree-Fock level partly on account of the large numbers of electrons they contain and partly because of the importance of relativistic effects. Hence, for such systems, it appears that the Slater-Kirkwood formula will have to be used for the foreseeable future. It should be pointed out that the values for $C_6(XY)$ coefficients which had been calculated using the Slater-Kirkwood formula before the work of Fowler *et al.* [49] are seriously in error either because inappropriate values for the electron numbers were employed or because incorrect values were used for the ionic polarizabilities. This earlier unreliable work has been fully discussed elsewhere [49].

4. AVOIDANCE OF DENSITY FUNCTIONAL DESCRIPTIONS OF THE UNCORRELATED POTENTIALS

4.1 Overview

A number of different variants of density functional theory have been used to calculate the interaction energies of closed shell atoms and ions since this method was suggested by Lenz and Jensen (see Gombas [68]) and first applied numerically by Massey and Sida in 1955 [69,70]. The variant often known as the Gordon-Kim method differs from that of Massey and Sida solely by introducing a contribution from the correlation energy. This method has been extensively used (e.g. [10,19,71–75]) to investigate ionic solids since its first application to study the interaction of pairs of rare gas atoms [8].

It is the Hohenberg-Kohn theorem [76] which, from a modern perspective, provides the theoretical justification for trying to develop and refine density functional theory. This theorem states that the energy of any system of electrons is a unique functional of the electron density distribution. This provides the rationalization for the basic idea behind current calculations based on density functional theory which is to express the total electronic energy as an integral over all space of local energy contributions which are determined solely by the local electron density and its gradients. In the density functional approach, the uncorrelated short range interaction $V^0_{sXY}(x_{XY}R)$ is decomposed into coulomb $V^{coul}_{sXY}(s_{XY}R)$, kinetic energy $V^{ke}_{XY}(x_{XY}R)$ and exchange $V^{ex}_{XY}(x_{XY}R)$ contributions so that

$$V^0_{sXY}(x_{XY}R) = V^{coul}_{sXY}(x_{XY}\mathrm{R}) + V^{ke}_{XY}(x_{XY}R) + V^{ex}_{XY}(x_{XY}R) \qquad (32)$$

The coulomb term, which is the purely electrostatic contribution to $V^0_{sXY}(x_{XY}R)$ that would arise in the absence of any exchange of electrons between ion X and ion Y, is calculated exactly. This term is quite different from the point coulomb $q_Xq_Y/(x_{XY}R)$ contribution to the total uncorrelated interaction $V^0_{XY}(x_{XY}R)$. Thus $V^{coul}_{sXY}(x_{XY}R)$ is that part of the non-exchange electrostatic interaction remaining after the point coulomb term has been subtracted. $V^{coul}_{sXY}(x_{XY}R)$ is therefore a short range term which is only non-zero when the overlap of the densities of the two ions is not negligible. For realistic ionic separations $V^{coul}_{sXY}(x_{XY}R)$ is usually an order of magnitude smaller than $V^0_{sXY}(x_{XY}R)$. The exchange term $V^{ex}_{XY}(x_{XY}R)$ arises from that part of the electron–electron repulsion which involves the exchange of electrons between the ions. Both the kinetic energy and exchange contributions to $V^0_{sXY}(x_{XY}R)$ are computed using the density functional approach as the difference between the kinetic (exchange) energy in the interacting pair and the sum of the kinetic (exchange) energies of the non-interacting ions both having the non-stationary wavefunctions optimal for the crystalline environment. Since the Hohenberg-Kohn theorem shows that these energies are uniquely defined by the electron density, these are given by

$$V^g_{XY}(x_{XY}R) = \int\{E^g[\varrho_T(\mathbf{r})] - \mathrm{E}^g[\varrho_X(\mathbf{r})] - E^g[\varrho_Y(\mathbf{r})]\}d\mathbf{r} \tag{33}$$

where g denotes the type of contribution, thus being ke for the kinetic energy and ex for the exchange term. The quantities $E^{ke}[\varrho(\mathbf{r})]$ and $E^{ex}[\varrho(\mathbf{r})]$ are the kinetic and exchange functionals whose values at the position $\mathbf{r}$ are determined by the behaviour of the electron density $\varrho(\mathbf{r})$. The notation used should not be taken to imply that these functionals are necessarily determined solely by the value of $\varrho(\mathbf{r})$, it being possible that the gradients or maybe some other properties of the electron density are required to define these functionals completely. In (33) $\varrho_X(\mathbf{r})$ and $\varrho_Y(\mathbf{r})$ are the electron densities of the isolated ions X and Y in their non-stationary states whilst $\varrho_T(\mathbf{r})$ is the total electron density originating from the pair of ions when these are separated by the distance $x_{XY}R$. It is a computationally trivial matter to generate the densities $\varrho_X(\mathbf{r})$ and $\varrho_Y(\mathbf{r})$ of the non-interacting ions from the appropriate wavefunctions.

Although the Hohenberg-Kohn theorem shows that the expression (33) for both the kinetic and exchange contributions to the interaction energy is formally exact, its implementation is necessarily approximate not only because the exact electron densities are not available but also because the precise forms of the functionals $E^{ke}[\varrho(\mathbf{r})]$ and $E^{ex}[\varrho(\mathbf{r})]$ are not known. For the closed shell systems of interest here, the density $\varrho_T(\mathbf{r})$ of the interacting pair has almost invariably been taken to be the sum of the densities of the individual ions, so that

$$\varrho_T(\mathbf{r}) = \varrho_X(\mathbf{r}) + \varrho_Y(\mathbf{r}) \tag{34}$$

Evidence for the accuracy of this approximation has been reviewed in detail elsewhere [5,9]. The functionals $E^{ke}[\varrho(\mathbf{r})]$ and $E^{ex}[\varrho(\mathbf{r})]$ have often been approximated by assuming that the electron density of the system of interest varies sufficiently slowly in space that at each point the functionals can be taken to equal those for a non-relativistic infinite electron-gas having a uniform density equal to that of the electron density of the system at that point in space [77]. This approximation has been used in the vast majority of calculations based on density functional theory including all applications to ionic solids. In this case, the functionals are given by

$$E^{ke}[\varrho(\mathbf{r})] = F^{ke}(3/10)\,(3\pi^2)^{2/3}\,[\varrho(\mathbf{r})]^{5/3} \tag{35}$$

$$E^{ex}[\varrho(\mathbf{r})] = F^{ex}(-3/4)\,(3/\pi)^{1/3}\,[\varrho(\mathbf{r})]^{4/3} \tag{36}$$

with the parameters F^{ke} and F^{ex} both equal to unity. However evidence accumulated rapidly [56,78–83] which showed that the original implementation of density functional theory by Gordon and Kim [8] was not completely satisfactory because this usually underestimated the repulsion by a factor of between two and three for realistic interatomic separations. The most clearcut demonstration of this failure is provided by comparing [83] the interaction energies $V^0_{sXY}(x_{XY}R)$ calculated using the RIP programme with those computed using density functional theory, typical results being presented in Table 10. It can be seen that almost all of the repulsions calculated using the original Gordon and Kim method [8] and presented in the fifth column of interaction energies in Table 10 are smaller by factors of about two than those computed using the RIP programme [83]. The properties of ionic crystals predicted by Kim and Gordon [71] using the original Gordon and Kim method [8] and wavefunctions of the free isolated ions were in fair agreement with experiment because the errors introduced by using free ion wavefunctions and neglecting all short range interactions excepting that within the closest cation–anion pairs partially masked the shortcomings of the original Gordon and Kim method [8]. Thus the underestimation of the uncorrelated short range repulsions $V^0_{sXY}(x_{XY}R)$ introduced by using the original Gordon and Kim approach [8] for $V^0_{sCA}(R)$ and neglecting $V^0_{sAA}(x_{AA}R)$ and $V^0_{sCC}(x_{CC}R)$ were partially cancelled by the overestimation of $V^0_{sCA}(R)$ introduced by using free ion wavefunctions.

Although the Hohenberg-Kohn theorem [76] shows that there exist exact kinetic energy and exchange functionals, those (35) and (36) will be in error for two different but related reasons. Firstly these two functionals are only correct if the electron density is constant throughout space which is clearly not the case in an actual atom or ion. Secondly the functionals (35) and (36) are only exact not only if the electron density is constant but also only if the system is infinite in extent. In particular for a system containing a finite rather than an infinite number of electrons, the exchange functional (36) is too large in magnitude because it includes a spurious self exchange contribution [78,79].

One can attempt to rectify the erorrs arising from using the functionals for a uniform electron gas by trying to express each of the unknown exact funtionals as a Taylor series expansion in the local electron density. This procedure introduces into (35) and (36) additional terms which involve the gradients of the density $\varrho(\mathbf{r})$ [84–86]. However the results calculated by introducing into the original Gordon and Kim method [8] the leading gradient correction to the kinetic energy functional are seen (sixth column of interaction energies in Table 10) to be in even greater disagreement with the exact results (the RIP predictions in Table 10) than those derived without introducing this correction. Furthermore introduction of this gradient correction to one of the two most satisfactory modifications of density functional theory, namely that due to Lloyd and Pugh [56] discussed below, completely destroys (see third column of interaction energies in Table 10) the fair agreement (Table 10 second column of interaction energies) between the exact results and the predictions of this method before the introduction of the gradient correction. It has been shown in a more extensive study of gradient corrections described in [85] that these shortcomings could not be rectified either by considering further terms in the gradient expansion of the kinetic energy functional or by introducing gradient corrections into the exchange functional. It was further shown that these difficulties arose because the gradient expansion is only convergent in regions of space where both the conditions (37)

Table 10 Comparison of inter-atomic potentials computed using different variants of density functional theory with predictions of the RIP programme[1]

Atom[2]	*R*	*RIP (exact)*[3]	*predictions of density functional theory*[4] *Lloyd and Pugh*[5]		*MWG*[6]	*unmodified*[7]	
			no grad	*grad*	*no grad*	*no grad*	*grad*
Ne	3.0	0.1043	0.1256	0.0642	0.1178	0.0939	0.0325
Ne	4.0	0.0089	0.0128	−0.0042	0.0107	0.0076	−0.0094
Ar	3.0	0.9634	0.5871	0.4576	0.5612	0.4115	0.2820
Ar	4.0	0.1589	0.1320	0.0740	0.1169	0.0824	0.0244
Ar	5.0	00252	0.0260	0.0027	0.0206	0.0131	−0.0201

[1]All energies in atomic units computed taking the wavefunction for the interacting pair to be an anti-symmetrized product of the non-relativistic Hartree-Fock wavefunctions of the isolated atoms. Electron correlation is not considered. R is inter-atomic distance in a.u.
[2]Calculated interaction energies for a homonuclear pair of the indicated atoms.
[3]From Wood and Pyper [83], interaction energy which is exact for the given wavefunction.
[4]no grad denotes use of the kinetic energy functional (35) without introducing gradient corrections. grad denotes computed with the addition of the gradient corrections to this functional. grad results derived by adding the gradients corrections computed by Shih [84] to the no grad results. These corrections obtained as the differences between the grad and non grad results of Shih [84].
[5]Lloyd and Pugh variant [56], results from Wood and Pyper [83].
[6]MWG is Modified Waldman-Gordon variant [80]. Uses the values of the kinetic and exchange correction factors F^{ke} and F^{ex} derived for Ne.
[7]Unmodified density functional method [8] with correction factors F^{ke} and F^{ex} set to unity, results from Wood and Pyper [83].

involving the ratio of the modulus ($|\nabla\varrho(\mathbf{r})|$) of the gradient of the density to a certain function of the density are satisfied.

$$|\nabla\varrho(\mathbf{r})/[\varrho(\mathbf{r})(3\pi^2\varrho(\mathbf{r}))^{1/3}] < 1 \tag{37a}$$

$$|\nabla_i\nabla_j\varrho(\mathbf{r})|/[|\nabla\varrho(\mathbf{r})|\ (3\pi^2\varrho(\mathbf{r}))^{1/3}] < 1 \tag{37b}$$

It was shown [85] that these conditions are violated for a very large fraction of the outer spatial regions in an atom which are the very regions which make the overwhelming contributions to the density functional predictions (33) of the interaction energy. This explains the unsatisfactory results obtained when the gradient expansions of the functionals (35) and (36) are applied in all the spatial regions contributing to the integrals in (33). A modified variant of the gradient expansion was therefore proposed [85] in which the gradient terms are introduced only in those spatial regions where the conditions (37) are satisfied. However it was tested for only two systems, namely for the interaction of two helium atoms and for that of two neon atoms. Although it eliminated the unsatisfactory features of previous interaction energy calculations using gradient expansions, the results were little different from those generated by the two most reliable variants of density functional theory, the LP and MWG approaches discussed below, in which gradient terms are not introduced. Both these two variants give a good account of these two systems. It would be most interesting to apply the modified gradient expansion method [85] to that system, namely AgF, for which even these two variants of density functional theory fail [4,83]. The violation of the conditions (37) with the consequent inability to apply gradient expansions in those outer atomic spatial regions making the largest contribution to the interaction energy might well prevent this approach from rectifying the deficien-

cies shown by density functional theory for this system. It is also of interest that the gradient expansion approach [85] has not been used in the latest work [74,75] on ionic solids to employ density functional theory, the older Waldman-Gordon variant [80,81] discussed in section 4.3 being retained in this later work. Here gradient corrections will not be further considered not only because one can anticipate problems caused by the inability to use them where the conditions (37) are violated but also because they have not so far been applied to ionic solids.

Currently there are two different modifications of the original Gordon-Kim method [8] that are to be preferred over other variants. The kinetic and exchange functionals (35) and (36) appropriate to a uniform electron gas are the basis for both of these, the two variants being distinguished through the choice of the correction factors F^{ke} and F^{ex}.

4.2 The Lloyd And Pugh Variant

The first two variants of density functional theory which appear to be preferrable to other approaches is that (LP) due to Lloyd and Pugh [56]. In this method, which is a slight modification of that introduced by Rae [78,79], the kinetic energy functional is used unmodified so that F^{ke} is taken to be unity. The LP variant is distinguished by taking the exchange correction factor F^{ex} to equal the parameter $\gamma(N_e)$ where N_e is the sum of the numbers of outermost electrons on the two interacting species. The parameter $\gamma(N_e)$ is obtained [78,79] by rederiving the exchange energy of a uniform electron gas explicitly eliminating the self exchange of the number N_e of electrons that are considered to contribute significantly to the exchange component of the interaction energy $V_{XY}^{ex}(x_{XY}R)$. The elimination of the spurious self-exchange reduces the magnitude of the exchange contribution $V_{XY}^{ex}(x_{XY}R)$ predicted by the original method [8] so that the parameter $\gamma(N_e)$ is less than unity. This parameter decreases as N_e decreases becoming zero for $N_e = 2$ and tending to unity in the limit of infinite N_e.

The LP variant is distinguished from other variants in which F^{ex} is taken to equal $\gamma(N_e)$ by the particular choice made for N_e. There is more than one variant using a Rae style ($F^{ex} = \gamma(N_e)$) exchange correction factor because N_e can be taken to be either, as originally suggested [78], the total number or, as later suggested [56], the number of outermost electrons on both atoms. There are four such variants [82] because, since the same $\gamma(N_e)$ has to be used for both the interacting system of two atoms as well as for the separated atoms, the question arose as to whether N_e should be calculated from the number of electrons on both [78] or, as argued subsequently [79], from the number on just one atom. This question has been considered [82,83] and it was concluded that N_e should be taken to be the number of outermost electrons on both atoms, the recommendation of Lloyd and Pugh [56]. This conclusion was reached both by comparing the density functional predictions of the binding energies and equilibrium interatomic separations of the inert gas dimers with experiment [82] and by comparing the density functional predictions of the uncorrelated interactions with their RIP counterparts [83]. The Lloyd and Pugh [56] prescription for selecting N_e is also supported by purely theoretical arguments. Thus it is clearly dubious to include the inner electrons in the calculation of N_e because such electrons do not contribute to the interaction beyond screening the appropriate number of units of nuclear charge. In particular it has been shown [56,82] that the inner electrons do not contribute to the exchange interaction energy $V_{XY}^{ex}(x_{XY}R)$ so that it is illogical to correct this with a $\gamma(N_e)$ calculated from a value of N_e which includes these inner electrons. The choice

for N_e of the number of outermost electrons on just one atom has the very curious consequence that $V_{XX}^{ex}(x_{XX}R)$ is predicted to vanish for the interaction of two helium atoms because $\gamma(2)$ is zero [83]. Since there must be an exchange contribution to the energy of interaction of two helium atoms, the vanishing of this quantity when N_e is chosen to be the number of outer electrons on just one atom provides further strong evidence that this choice for N_e is not satisfactory.

The results presented in the second column of interaction energies in Table 10 show that the LP modification largely removes the significant discrepancies between the predictions of the original method [8] and the RIP calculations. These results are typical of those found [83] for pairs of rare gas atoms in that the LP method reproduces the RIP results quite well at intermediate distances but, for the heavier systems, underestimates the repulsion at shorter distances.

4.3 The Modified Waldman-Gordon Variant

The only other variant of density functional theory of comparable reliability to the LP approach is a modification of that due to Waldman and Gordon [80,81]. In the Waldman-Gordon (WG) modification both the kinetic and exchange contributions to the interaction energy are scaled by factors F^{ke} and F^{ex} which are derived from a Hartree-Fock calculation for one neutral atom having the same number of electrons as the total number on both the interacting species. The factors F^{ke} and F^{ex} are taken to equal the ratio of the total kinetic or exchange energy computed from atomic Hartree-Fock theory to the corresponding total energy that is predicted when the same Hartree-Fock electron density function is used as input to the functionals (35) and (36) appropriate to an infinite uniform electron gas where $F^{ke} = F^{ex} = 1$. Since the exchange correction factors are found to be less than unity [80] and to decrease as the number of electrons decreases, it would appear that their physical origins are at least partially the same as those of the Rae style ($F^{ex} = \gamma(N_e)$) correction factors introduced to eliminate spurious self-exchange contributions. The kinetic energy correction factors F^{ke} are found [80] to be slightly greater than one, being 1.125 for the interaction of two Helium atoms, and to decrease towards unity as the number of electrons increases.

The Waldman-Gordon method would appear to be highly reasonable for systems in which all the electrons are in outer shells. Such systems naturally have only a small number of electrons in total. However the WG method for deriving correction factors is objectionable for systems having a large number of core electrons because these contribute only negligibly to the interaction energy whilst making the overwhelming contributions to the total atom energies used to derived F^{ke} and F^{ex}. Indeed for heavy atoms both F^{ke} and F^{ex} are close to unity because for the inner core orbitals, which are the dominant contributors to the total atom energies, the difference between the Hartree-Fock and density functional predictions of the kinetic (exchange) energy is only a very small fraction of the total kinetic (exchange) energy. The prediction of correction factors F^{ke} and F^{ex} close to unity causes the interaction energies computed using them to differ only very slightly from those calculated using the original Gordon-Kim method [8] which is now known to seriously underestimate the repulsion. This explains why the properties of several crystals containing ions of intermediate nuclear charge appeared to be satisfactorily predicted by the WG method [87] even though free ion wavefunctions were used and the inter-ionic dispersive attractions were entirely neglected. The underestimation of the short range repulsion by the

original Gordon-Kim method [8] to which the WG variant reduces when F^{ke} and F^{ex} approach unity clearly cancelled the errors introduced by using free ion wavefunctions and neglecting the dispersion. The WG correction factors for ions of low nuclear charge do not suffer from the deficiency of reducing to unity on account of the large numbers and high binding energies of the core electrons. This is certainly one of the factors which explains why the later results of Gordon and coworkers [19,74,88] are more satisfactory. Since no crystals containing ions of high nuclear charge were considered not only were the WG correction factors more reasonable but also the neglected dispersive attractions would not be so large. Furthermore the modifications of the ion wavefunctions caused by the crystalline environment were considered.

It has just been shown that the original WG approach [80] is not satisfactory for heavy ions because these have tightly bound cores containing many electrons. However for light ions these drawbacks of the original WG method are absent. This suggests that the Waldman-Gordon method would be satisfactory if modified by deriving the correction factors from the atom having the same number of electrons as just the total number of outermost electrons on the two interacting species. It is this modification, to be called the modified Waldman-Gordon (MWG) variant that was used in all the calculations labelled WG in [4] as well as in all those discussed in this talk. The results presented in the fourth column of interaction energies in Table 10 show that the MWG approach performs as well as the LP variant in considerably reducing the discrepancies between the RIP results and the predictions of the original density functional method [8].

4.4 *Anion–Anion Interactions*

There has been much interest in computing the inter-ionic potentials governing the interaction of an anion with its closest anion neighbours because these quantities cannot be readily extracted from empirical fits to experimentally determined crystal properties [4,72]. The uncorrelated parts $V^0_{sAA}(x_{AA}R)$ of these interactions have been computed using density functional theory [10,19,72–75,87,88] non-relativistic *ab-initio* quantum chemistry methods [89,90] and the RIP programme [4]. The non-relativistic quantum chemistry calculations, whose reliability has been reviewed elsewhere [5], will not be considered here since the present objective is to examine the reliability of density functional theory by comparing its predictions with those generated using the RIP programme.

Density functional theory has been used quite extensively to compute the uncorrelated halide–halide interactions. Although free ion wavefunctions were used in the earliest of such work, [72,87], the influence of the environment was considered in later studies [19,88]. It is interesting to realize that the modifications of the ion wavefunctions caused by the crystalline environment will vary significantly from crystal to crystal if the differences between the free and in-crystal wavefunctions are appreciable. In this event, these variations of the in-crystal anion wavefunctions will be propogated into the computed halide-halide potentials $V^0_{sXX}(x_{XX}R)$ with the consequence that there no longer exists one unique potential $V^0_{sXX}(x_{XX}R)$ for each halide ion X, this potential being different in each crystal. In the model (19) for the environmental potential acting on an anion electron, the differences in the halide ion wavefunctions between one crystal and another arise through changes in the constants ϕ_{envA} and R_0. For different crystals having the same structure, the constant ϕ_{envA} remains unchanged so that for the same value of R the differences in the halide ion wavefunctions arise

from the changes in the parameter R_0. Since numerically R_0 is equal to the radius of the counter cation, the halide wavefunctions for a given value of R become increasingly compressed by the environment as the size of the cation increases. The short range interactions predicted using density functional theory depend directly on the existence of spatial regions in which the electron densities of both the interacting ions are simultaneously non-zero. Hence for a fixed value of R and a given crystal structure one expects the uncorrelated short range halide-halide interactions predicted using density functional theory to become increasingly repulsive as the size of the cation decreases. This is illustrated by the computations reported in Table 11 for the interaction of two fluoride ions separated by a distance $4\sqrt{2}$ a.u. in crystals having the NaCl structure and a fixed R of 4.0 a.u.. Thus the size of the fluoride ion at this fixed F^- ..F^- separation of $4\sqrt{2}$ a.u. decreases on passing from the free anion through that in LiF and NaF to the most compact in AgF since the size of the cations increases on traversing this series. Consequently both the LP and MWG variants of density functional theory predict these repulsions to decrease along this sequence.

The RIP programme can be used to compute the uncorrelated short range halide-halide interactions once wavefunctions suitably adapted to the crystalline environment have been generated. The resulting potentials have been presented in detail in Appendix 5 of [4] where they are compared with those predicted using the LP and MWG variants of density functional theory. The RIP calculations of the uncorrelated short range F^- ..F^- interactions presented in Table 11 show how for a fixed R of 4.0 a.u. the differences in the fluoride ion wavefunctions really do affect these potentials. The results show that this potential increases from being attractive for two free F^- ions to become increasingly repulsive as the size of the counter cation increases. Since the RIP calculations are exact once the ion wavefunctions are given, the differences between the RIP results and the predictions of density functional theory uncover the limitations of the latter approach since, for a given cation, the same fluoride ion wavefunction is input to both the density functional and the RIP calculations. The LP and MWG variants of the density functional method both fail to reproduce the attraction between two free F^- ions and fail to reproduce the increase of the repulsion as the anions become more contracted. The electron density distribution of an anion is comparatively diffuse so that it is plausible to attribute the increase of the repulsion to the electron density distribution becoming more compact and in some sense 'harder', this increasing compactification more than offsetting the decrease of the orbital overlaps. The density functional method naturally can take into account

Table 11 Comparison of uncorrelated F^- ..F^- interactions for $R = 4.0$ a.u.[1]

	Method[2]	*F^- ion wavefunction*[3]			
		free	*in LiF*	*in NaF*	*In AgF*
$V^0_{sAA}(4\sqrt{2})$	Dens funct LP	0.00395	0.00272	0.00218	0.00199
	Dens funct MWG	0.00228	0.00161	0.00128	0.00116
	RIP (exact)[4]	−0.00014	0.00095	0.00118	0.00127

[1] From [4]; all energies in a.u.
[2] Dens funct LP and Dens funct MWG denote the Lloyd and Pugh [56] and modified Waldman-Gordon variants of density functional theory.
[3] F^- ion wavefunctions computed using the model (19) to describe the influence of the crystalline environment on the anion electrons.
[4] Uncorrelated short range potential which is exact for the F^- ion wavefunctions used.

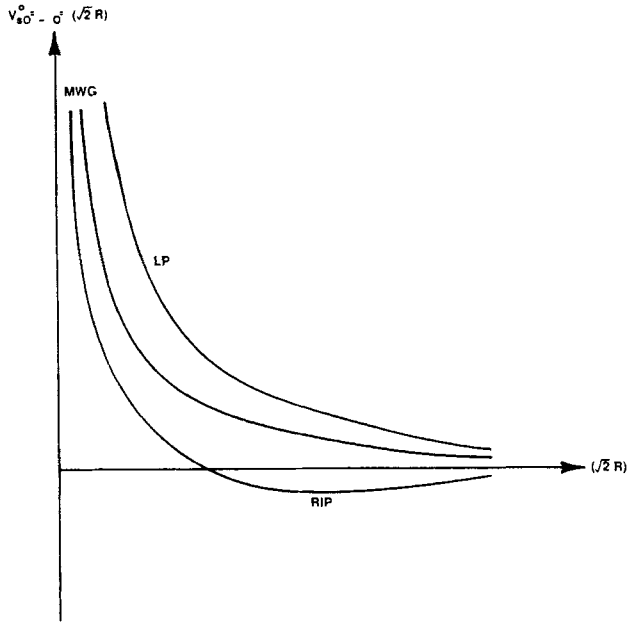

Figure 8 Comparison of the RIP and Lloyd and Pugh (LP) and modified Waldman-Gordon (MWG) density functional predictions of the uncorrelated short range interaction within the closest pairs of oxide ions in MgO.

only the latter factor. For cation–anion interactions, however, the contraction of the anion decreases the uncorrelated short range repulsion as illustrated by the results presented in Table 4 and discussed in section 2.2(ii).

The uncorrelated short range interactions $V^0_{sAA}(\sqrt{2}R)$ between the closest pairs of oxide ions in MgO have been computed [4] using both LP and MWG variants of density functional theory. The two resulting potentials are compared in Figure 8 with the predictions [4] derived using the RIP programme. The same set of oxide ion wavefunctions was used in all three computations so that the discrepancies between the density functional and RIP results display the shortcomings of the former. Both variants of density functional theory not only overestimate the repulsion for $R < 4.25$ a.u. but also fail to reproduce the small attractive tail occuring at larger R. These discrepancies are of more than purely academic interest because the values of 2878 kJ mole^{-1} and 2936 kJ mole^{-1} for the MgO lattice energy predicted from (14) using these two variants of density functional theory to compute $V^0_{sO^{--}\cdot O^{--}}(\sqrt{2}R)$ but retaining the RIP $V^0_{sMg^{++}\cdot O^{--}}(R)$ should be compared [4] with the experimental result of 3038 kJ mole^{-1}. The lattice energy of 3020 kJ mole^{-1} predicted [4] from the full RIP calculation is in considerably better agreement with experiment. The full RIP calculation differs from the above two density functional ones solely in using the RIP rather than the density functional predictions of the O^{--} ..O^{--} uncorrelated short range interaction.

4.5 Comparison Of Density Functional and RIP Predictions Of Crystal Cohesion

The calculations just described demonstrated that even the two most reliable variants of density functional theory failed to reveal some of the subtle details of the anion–

anion interactions. The significance of the inaccuracies in the density functional results for all three uncorrelated short range potentials $V^0_{sCA}(R)$, $V^0_{sCC}(x_{CC}R)$ and $V^0_{sAA}(x_{AA}R)$ can be elucidated by comparing the crystal properties predicted from these potentials with those derived by the method which differs solely in using uncorrelated short range interactions computed using the RIP programme. It is thus necessary to use the same ion wavefunctions as input to both the density functional and RIP calculations and to include in both the short range correlation energy in the usual density functional approximation [8] as well as the damped dispersion energy (26)–(28). There is, in principle, an inconsistency with the density functional calculations in using the non-relativistic functionals (35) and (36) if relativistic ion wavefunctions are used. However it has been shown [42] that substitution of the relativistic kinetic energy functional for the non-relativistic one (35) scarcely changed the predicted inter-atomic potential even for the interaction of two Hg atoms. This result is not inconsistent with the finding, discussed in section 1.2, that the direct relativistic effect significantly modifies the behaviour of valence *s* electrons in such heavy elements. Although the motion of such electrons is quite relativistic in the inner spatial regions, these electrons will have low momenta in the outer spatial regions which yield the dominant contributions to the density functional predictions (33) of the interaction energy. Hence, provided that the correct relativistic electron densities are employed, the use of non-relativistic rather than relativistic functionals only minimally affects the density functional predictions which are thus suitable for comparison with fully relativistic RIP calculations.

For all six ionic crystals examined in the study [4], the predictions of both the LP and MWG variants of density functional theory were compared with the corresponding ones derived using the RIP programme. The conclusions which emerged from this study are illustrated by the typical results that are assembled in Table 12. Even for the systems for which the density functional approach works quite well, it is seen not only that the predictions of both the LP and MWG methods differ significantly from those derived using the RIP programme but also that the RIP results agree significantly better with experiment. Even for a system such as LiF, the results in Table 12 flatter density functional theory in that the agreement with experiment of both the LP and MWG calculations arises at least partially through cancellation of errors. Thus examination of the uncorrelated short range potentials presented in Appendix 5 of [4] shows that both these density functional approaches underestimate the $Li^+ ..F^-$ short range repulsion whilst overestimating that within the closest pairs of F^- ions. Similar cancellations of errors in both the LP and MWG methods have been uncovered for other systems [4]. In particular the results presented in Appendix 5 of [4] show that the uncorrelated short range interaction between two Pb^{++} ions is predicted very poorly by density functional theory as is that between two Ag^+ ions. Thus the LP method underestimates the uncorrelated short range $Pb^{++} ..Pb^{++}$ repulsion by a factor of two whilst underestimating that between two Ag^+ ions by a factor of four. The MWG variant predicts even less repulsion than the LP method. Perhaps the most striking conclusion to emerge from Table 12 is that both the LP and MWG methods fail completely for AgF. This failure occurs because the uncorrelated short range $Ag^+ ..F^-$ repulsion is seriously overestimated for the reasons which have been described elsewhere [83].

The data assembled in Tables 11 and 12 is sufficient for the current status of density functional theory to be assessed. It is now quite clear that Gordon and Kim's [8] implementation of density functional theory is not satisfactory in the form originally presented in that paper. Furthermore nothing very useful has so far emerged by

Table 12 Comparison of density functional and RIP predictions of crystal properties[1,2]

	LiF				*AgF*				PbF_2			
	Dens funct[3,5]		*RIP*[4]	*expt*[5]	*Dens funct*		*RIP*	*expt*	*Dens funct*		*RIP*	*expt*
	LP[6]	*MWG*[7]			*LP*	*MWG*			*LP*	*MWG*		
D_e	1044	1081	1038	1036	786	819	944	942, 953	2355	2433	2433	2491
R_e	3.86	3.77	3.89	3.81	5.37	5.22	4.64	4.66	5.08	4.97	4.87	4.86
B	8.00	9.29	8.16	6.98–8.67	2.59	3.44	6.37		5.89	6.77	6.56	6.53

[1] All results from [4] and computed from expression (14) for $U_L(R)$ thus including both the short range correlation term $V_{sXY}^{corr}(x_{XY}R)$ computed as in [8] and the damped dispersion energy $U_{disp}(R)$ (26).
[2] All results for lattice energies D_e in kJ mole^{-1}, closest equilibrium cation–anion separations R_e in a.u. and bulk compressibilities B in 10^{12} Nm^{-2}).
[3] Dens funct means all these potentials computed using density functional theory.
[4] RIP means all uncorrelated short range potentials computed using the RIP programme.
[5] See [4] and [5] for sources of experimental results.
[6] Lloyd and Pugh variant [56].
[7] MWG is Modified Waldman-Gordon variant. Uses the values of the kinetic and exchange correction factors F^{ke} and F^{ex} derived by considering only the outermost electrons.

considering expansions in the gradients of the electron density. It would appear that only the Lloyd and Pugh [56] and Modified Waldmann-Gordon variants of density functional theory are currently worthy of consideration. The comparison (Table 12) of RIP and density functional predictions of crystal properties as well as the discussion of the uncorrelated short range anion–anion potentials presented in the last section all show that appreciable errors can be introduced by using density functional theory even in its two best variants. Even for a potential $V^0_{sXY}(x_{XY}R)$ well predicted by density functional theory, it is interesting to realize that the individual kinetic ($V^{ke}_{XY}(x_{XY}R)$) and exchange ($V^{ex}_{XY}(x_{XY}R)$) components calculated using either the LP or MWG variants are often an order of magnitude smaller than their exact counterparts computed using the RIP programme [83] as is the case for the interaction of two Radon atoms separated by 6.0 a.u.. However the magnitudes of these discrepancies depend on both the interacting species as well as on their separation. Thus for the Na^+ ..F^- interaction derived using the environmental models (19) and (21) to compute the wavefunctions, the true kinetic energy contributions to the interaction energies at R = 3.0 a.u. and 4.5 a.u. of 0.841 a.u. and 0.0537 a.u. are greater than the density functional predictions of 0.1862 a.u. and 0.0107 a.u. by factors of 4.5 and 5.0 respectively. The significance and implications of these results are not at present clear but in view of the size of the discrepancies it is not unreasonable to expect that useful insights might be gleaned from further study of this matter. It can be concluded that one should avoid using density functional theory to compute the uncorrelated short range repulsions if a more accurate method, such as for example computation with the RIP programme, is available.

5. CONCLUSION

The aim of this talk has been to discuss four different factors which need to be considered in non-empirical studies of the properties of ionic solids. Since it is not the aim here to give a comprehensive review of such calculations, the references have been given as an aid for the reader to find further details and not as part of a historical survey. Hence I offer no apologies for omitting references to earlier and more fundamental pieces of work if a later but less original paper presents the same results more clearly. Any such omissions will be made good in the review [5].

It has been described how relativity modifies the properties of ions of high nuclear charge and how these modifications are reflected in the inter-ionic potentials. It has been shown that these effects are appreciable for ions having nuclear charges greater than those in the third series of transition elements for which perturbation treatments of relativity are inadequate. The relativistic effects in such systems are too large to ignore in calculations aiming to achieve a high precision.

The mechanisms through which the crystalline environment influences the electronic properties of ions, such as the polarizability, and hence the inter-ionic potentials have been described. Calculations using a simple yet physically realistic model for the crystalline environment showed that the environmentally induced modifications of the ion wavefunctions are too large to be ignored in calculations aiming for high precision.

The physical origins of the inter-ionic dispersive attractions have been outlined. It was pointed out that the most familiar form for such an attraction, the undamped dispersion energy in which the dipole–dipole interaction $-C_6(ab)(x_{ab}R)^{-6}$ appears as

the leading term, is only valid if the overlap of the wavefunctions of the interacting pair of ions is negligible. The results of an approximate but physically realistic theory for the damping of the dispersion energy when these overlaps are appreciable demonstrated that such damping is too large to be ignored. The importance of using reliable values for the dispersion coefficients, particularly the $C_6(XY)$ coefficients, was stressed and a procedure for deriving trustworthy $C_6(XY)$ values presented. A cautionary note was sounded concerning many of the values previously reported in the literature.

The reliability of different variants of the density functional method for computing inter-ionic potentials has been discussed and it was shown that even the two most reliable variants, namely the Lloyd and Pugh (LP) and Modified Waldman-Gordon (MWG) methods, have weaknesses about which it would be foolhardy to remain in ignorance. Thus the density functional predictions of the closest cation–cation and closest anion–anion interactions can be so poor that they bear little relation to the actual potentials for these ion pairs. The density functional predictions of the properties of many crystals do not suffer from similar failures provided that this gives a reasonable account of the closest cation–anion interaction. However even in this event non-negligible errors are introduced by substituting density functional predictions of the uncorrelated short range potentials for their RIP counterparts which are exact once the ion wavefunctions have been specified. For some systems, such as AgF, any variant of density functional theory currently available fails badly.

The four factors described in this talk will need to be considered in all future work on ionic crystals even though improvements will doubtless be made in the approximations described here.

Acknowledgement

I thank Dr. A. M. Stoneham (AERE Harwell) for a private communication concerning the early history of density functional calculations of inter-ionic potentials. I also thank Mr C. Pike and Dr D. M. Holton (University Chemical Laboratory Cambridge) for reading the manuscript.

References

[1] C.R.A. Catlow and W.C. Mackrodt, "Recent developments in simulation studies of ionic material", *Solid State Ionics*, **8**, 175 (1982).
[2] A.M. Stoneham, "Interatomic potentials for condensed matter", *Physica*, **131B**, 69 (1985).
[3] G.P. Srivastava and D. Weaire, "The theory of the cohesive energies of solids", *Adv. Phys.*, **36**, 463 (1987).
[4] N.C. Pyper, "Relativistic Ab-initio calculations of the properties of ionic solids", *Phil. Trans. Roy. Soc.*, **A320**, 107 (1986).
[5] N.C. Pyper, "Ab-initio calculations of inter-ionic potentials and the cohesive properties of ionic solids", *Adv. Solid State. Chem.*, **2** submitted (1989).
[6] N. Jacobi and Gy. Csanak, "Dispersion forces at arbitrary distances", *Chem. Phys. Letts.*, **30**, 367 (1975).
[7] A. Koide, "A new expansion for dispersion forces and its application", *J. Phys.*, **B9**, 3173 (1976).
[8] R.G. Gordon and Y.S. Kim, "Theory for the forces between closed shell atoms and molecules", *J. Chem. Phys.*, **56**, 3122 (1972).
[9] M.J. Clugston, "The calculation of intermolecular forces. A. critical examination of the Gordon-Kim model", *Adv. Phys.*, **27**, 893 (1978).
[10] A.J. Cohen and R.G. Gordon, "Modified electron-gas study of the stability, elastic properties and high pressure behaviour of MgO and CaO crystals", *Phys. Rev.* **B14**, 4593 (1976).
[11] I.V. Abarenkov and I.M. Antonova, "Interatomic interactions in alkali halides", *Phys. Stat. Solidi*, **38**, 783 (1970).

[12] R.N. Euwema, G.G. Wepfer, G.T. Surratt and D.L. Wilhite, "Hartree-Fock calculations for crystalline Ne and LiF", *Phys. Rev.*, **B9**, 5249 (1974).
[13] R. Dovesi, C. Ermondi, E. Ferrero and C. Pisani, "Hartree-Fock study of lithium hydride with the use of a polarizable basis set", *Phys. Rev.*, **B29**, 3591 (1984).
[14] V.R. Saunders, "Ab-initio Hartree-Fock calculations for periodic systems", *Farad. Symp. Chem. Soc.*, **19**, 79 (1984).
[15] R. Dovesi, C. Pisani, F. Ricca and C. Roetti, "Exact exchange Hartree-Fock calculations for periodic systems III. Ground state properties of diamond", *Phys. Rev.*, **B22**, 5936 (1980).
[16] W. von der Linden and P. Fulde, "Efficient approach to the ab-initio Hartree-Fock problem of solids with application to diamond and silicon", *Phys. Rev.*, **B34**, 1063 (1986).
[17] R. Dovesi, C. Pisani and C. Roetti, "Exact exchange Hartree-Fock calculations for periodic systems II. Results for graphite and hexagonal boron nitride", *Int. J. Quant. Chem.*, **17**, 517 (1980).
[18] R. Dovesi, C. Pisani, C. Roetti and P. Dellarole, "Exact exchange Hartree-Fock calculations for periodic systems IV. Ground state properties of cubic boron nitride", *Phys. Rev.*, **B24**, 4170 (1981).
[19] C.W. Muhlhausen and R.G. Gordon, "Electron-gas theory of ionic crystals including many body effects", *Phys. Rev.*, **B23**, 900 (1981).
[20] R. Boehm and J. Yaris, "Van der Waals forces including exchange in the small overlap region", *J. Chem. Phys.*, **55**, 2620 (1971).
[21] I.P. Grant, B.J. McKenzie, P.H. Norrington, D.F. Mayers and N.C. Pyper, "An atomic multiconfigurational Dirac-Fock package", *Comput. Phys. Comm.*, **21**, 207 (1980).
[22] C.P. Wood and N.C. Pyper, "Ab-initio relativistic lattice energy calculations for fluorides of the 7p series of superheavy elements", *Chem. Phys. Lets.*, **81**, 395 (1981).
[23] C.P. Wood and N.C. Pyper, "An ab-initio relativistic calculation for $(E113)_2$", *Chem. Phys. Letts.*, **84**, 614 (1981).
[24] C.P. Wood and N.C. Pyper, "Relativistic ab-initio calculations of interaction energies: Formulation and applications to ionic solids", *Phil. Trans. Roy. Soc.*, **A320**, 71 (1986).
[25] S.J. Rose, I.P. Grant and N.C. Pyper, "The direct and indirect effects in the relativistic modification of atomic valence orbitals", *J. Phys. B*, **11**, 1171 (1978).
[26] P.A.M. Dirac, "The Principles of Quantum Mechanics", Cambridge University Press, 1958, pp. 253–273.
[27] J.J. Sakurai, "Advanced Quantum Mechanics", Addison-Wesley, Reading Massachusetts, 1967, pp. 78–131.
[28] I.P. Grant, "Relativistic calculations of atomic structures", *Adv. Phys.*, **19**, 747 (1970).
[29] V.M. Burke and I.P. Grant, "The effect of relativity on atomic wavefunctions", *Proc. Phys. Soc.*, **90**, 297 (1967).
[30] D.F. Mayers, "Relativistic self-consistent field calculation for mercury", *Proc. Roy. Soc.*, **A241**, 93 (1957).
[31] B. Swirles, "The relativistic self-consistent field", *Proc. Roy. Soc.*, **A152**, 625 (1935).
[32] N.C. Pyper, P. Marketos and G.L. Malli, "Relativistic modifications of inter-ionic potentials in lead fluoride" *J. Phys. C*, **20**, 4711 (1987).
[33] N.C. Pyper, "Relativistic pseudopotential theories and corrections to the Hartree-Fock method", *Molec. Phys.*, **39**, 1327 (1980).
[34] N.C. Pyper, "First order perturbation treatments for relativistic pseudopotentials and corrections to the Hartree-Fock method I. Theory", *Molec. Phys.*, **42**, 1059 (1981).
[35] N.C. Pyper and P. Marketos, "First order perturbation treatments for relativistic pseudopotentials and corrections to the Hartree-Fock method II. Results", *Molec. Phys.*, **42**, 1073 (1981).
[36] N.C. Pyper and P. Marketos, unpublished work cited in N.C. Pyper, "Relativistic calculations for atoms, molecules and solids: Fully ab-initio calculations and the foundations of pseudopotential and perturbation theory methods", in Relativistic effects in atoms, molecules and solids, G.L. Malli, ed, Plenum, New York, 1983, NATO ASI series B, **87**, 437.
[37] J.D. Morrison and R.E.Moss, "Approximate solution of the Dirac equation using the Foldy-Wouthuysen hamiltonian", *Molec. Phys.*, **41**, 491 (1980).
[38] I.J. Keatley and R.E. Moss, "On the expectation values of relativistic corrections to the hamiltonian", *Molec. Phys.*, **49**, 1289 (1983).
[39] G.L. Malli and N.C. Pyper, "Ab-initio fully relativistic molecular calculations: bonding in gold hydride", *Proc. Roy. Soc.*, **A407**, 377 (1986).
[40] A.F. Ramos, N.C. Pyper and G.L. Malli, "Relativistic effects in bonding and dipole moments for the diatomic hydrides of the sixth-row elements", *Phys. Rev.*, **A38**, 2729 (1988).
[41] W. Kutzelnigg, "Basis set expansion of the Dirac operator without variational collapse", *Int. J. Quant. Chem.*, **25**, 107 (1984).

[42] N.C. Pyper, I.P. Grant and R.B. Gerber, "Relativistic effects on interactions between heavy atoms: The Hg–Hg potential", *Chem. Phys. Letts.*, **49**, 479 (1977).
[43] C.P. Wood and N.C. Pyper, "Relativistic corrections to carbon atom energy levels and their relation to the singlet-triplet splitting in methylene", *Molec. Phys.*, **41**, 149 (1980).
[44] P.W. Fowler and N.C. Pyper, "In-crystal polarizabilities derived by combining experimental and ab-initio results", *Proc. Roy. Soc.*, **A398**, 377 (1985).
[45] G.D. Mahan, "Polarizability of ions in crystals", *Solid State Ionics*, **1**, 29 (1980).
[46] P.W. Fowler and P.A. Madden, "The in-crystal polarizability of the fluoride ion", *Molec. Phys.*, **49**, 913 (1983).
[47] P.W. Fowler and P.A. Madden, "In-crystal polarizabilities of alkali and halide ions", *Phys. Rev.*, **B29**, 1035 (1984).
[48] P.W. Fowler and P.A. Madden, "In-crystal polarizability of O^{--}", *J. Phys. Chem.*, **89**, 2581 (1985).
[49] P.W. Fowler, P.J. Knowles and N.C. Pyper, "Calculations of two- and three-body dispersion coefficients for ions in crystals", *Molec. Phys.*, **56**, 83 (1985).
[50] P.W. Fowler and N.C. Pyper, "Dipole-quadrupole dispersion coefficients for ions in crystals", *Molec. Phys.*, **59**, 317 (1986).
[51] N.F. Mott and R.W. Gurney, "Electronic processes in ionic crystals", Oxford University Press, (1950).
[52] G.H.F. Diercksen and A.J. Sadlej, "Perturbation theory of electron correlation effects for atomic and molecular properties IV. Dipole polarizability of the fluoride ion", *Molec. Phys.*, **47**, 33 (1982).
[53] R.E. Watson, "Analytic Hartree-Fock solution for O^{--}", *Phys. Rev.*, **111**, 1108 (1958).
[54] E. Paschalis and A. Weiss, "Hartree-Fock-Roothaan Wavefunctions, electron density distribution, diamagnetic susceptibility, dipole polarizability and antishielding factor for ions in crystals", *Theoret. Chim. Acta*, **13**, 381 (1969).
[55] P.C. Schmidt, A. Weiss and T.P. Das, "Effect of crystal fields and self-consistency on dipole and quadrupole polarizabilities of closed shell ions", *Phys. Rev. B*, **19**, 5525 (1979).
[56] J. Lloyd and D. Pugh., "Some applications of a self-exchange corrected electron-gas model for intermolecular forces", *J. Chem. Soc. Farad II*, **73**, 234 (1977).
[57] H. Kreek and W.J. Meath, "Charge-Overlap Effects. Dispersion and Induction forces", *J. Chem. Phys.*, **50**, 2289 (1969).
[58] A. Dalgarno and J.T. Lewis, "The Representation of Long Range Forces by Series Expansions", *Proc. Phys. Soc.*, **69A**, 65 (1956).
[59] H. Jeffreys and B. Jeffreys, "Methods of Mathematical Physics", Cambridge University Press, 1946, p468.
[60] B.M. Axilrod and E. Teller, "Interaction of the van der Waals Type between Three atoms", *J. Chem. Phys.*, **11**, 299 (1942).
[61] P.W. Langhoff and M. Karplus, "Padé Approximants for Two- and Three-Body Dipole Dispersion Interactions", *J. Chem. Phys.*, **53**, 233 (1970).
[62] K.T. Tang, J.M. Norbeck and P.R. Certain, "Upper and Lower Bounds of two- and three- body dipole, quadrupole and octupole van der Waals coefficients for hydrogen, noble gas and alkali atom interactions", *J. Chem. Phys.*, **64**, 3063 (1976).
[63] J.C. Slater and J.G. Kirkwood, "The van der Waals Forces in Gases", *Phys. Rev.*, **37**, 682 (1931).
[64] G. Starkschall and R.G. Gordon, "Calculation of Coefficients in the Power Series Expansion of the Long-Range Dispersion Force between Atoms", *J. Chem. Phys.*, **56**, 2801 (1972).
[65] K.T. Tang, "Dynamic Polarizabilities and van der Waals Coefficients", *Phys. Rev.*, **177**, 108 (1969).
[66] W.C. Stwalley and H.L. Kramer, "Long-Range Interactions of Mercury Atoms", *J. Chem. Phys.*, **49**, 5555 (1968).
[67] G.D. Mahan, "van der Waals coefficients between closed shell ions", *J. Chem. Phys.*, **76**, 493 (1982).
[68] P. Gombas, "Statistische Behandlung des atoms", in Handbuch der Physik, Flugge, ed, Springer-Verlag, Berlin, 1956, **36**, 109.
[69] H.S.W. Massey and D.W. Sida, "Collision processes in meteor trials", *Phil. Mag.*, **46**, 290 (1955).
[70] D.W. Sida, "The scattering of positive ions by neutral atoms", *Phil. Mag.*, **2**, 761 (1957).
[71] Y.S. Yim and R.G. Gordon, "Theory of binding of ionic crystals: Application to alkali-halide and alkaline-earth-dihalide crystals", *Phys. Rev.*, **B9**, 3548 (1974).
[72] C.R.A. Catlow, K.M. Diller and M.J. Norgett, "Interionic potentials for alkali halides", *J. Phys. C*, **10**, 1395 (1977).
[73] W.C. Mackrodt and R.F. Stewart, "Defect properties of ionic solids: II Point defect energies based on modified electron-gas potentials", *J. Phys. C*, **12**, 431 (1979).
[74] M.D. Jackson and R.G. Gordon, "Electron-gas theory of some phases of magnesium oxide", *Phys. Rev.*, **B38**, 5654 (1988).

[75] G.H. Wolf and M.S.T. Bukowinski, "Variational stabilization of the ionic charge densities in the electron-gas theory of crystals: Applications to MgO and CaO", *Phys. Chem. Mineral.*, **15**, 209 (1988).
[76] P. Hohenberg and W. Kohn, "Inhomogeneous electron-gas", *Phys. Rev.*, **B136**, 864 (1964).
[77] N.H. March, W.H. Young and S. Sampanther, "The Many-body Problem in Quantum Mechanics", Cambridge University Press, 1967, Ch 5.
[78] I.A.M. Rae, "A theory for the interaction between closed shell systems", *Chem. Phys. Letts.*, **18**, 574 (1973).
[79] I.A.M. Rae, "A calculation of the interaction between pairs of rare gas atoms", *Molec. Phys.*, **29**, 467 (1975).
[80] M. Waldman and R.G. Gordon, "Scaled electron gas approximation for Intermolecular forces", *J. Chem. Phys.*, **71**, 1325 (1979).
[81] M. Waldman and R.G. Gordon, "Generalized electron gas – Drude model theory of intermolecular forces", *J. Chem. Phys.*, **71**, 1340 (1979).
[82] M.J. Clugston and N.C. Pyper, "A comparative study of Gordon-Kim interatomic potential theory variants: Application to the inert gases and mercury", *Chem. Phys. Letts.*, **63**, 549 (1979).
[83] C.P. Wood and N.C. Pyper, "Electron-gas predictions of interatomic potentials tested by ab-initio calculations", *Molec. Phys.*, **43**, 1371 (1981).
[84] C.C. Shih, "Inhomogeneity correction to the Thomas-Fermi Dirac model of rare gas diatomic systems", *Molec. Phys.*, **38**, 1225 (1979).
[85] E.W. Pearson and R.G. Gordon, "Local asymptotic gradient corrections to the energy functional of an electron gas", *J. Chem. Phys.*, **82**, 881 (1985).
[86] D.C. Langreth and M.J. Mehl, "Easily implementable non-local exchange-correlation energy functional", *Phys. Rev. Letts.*, **47**, 446 (1981).
[87] A.J. Cohen and R.G. Gordon, "Theory of the lattice energy, equilibrium structure, elastic constants and pressure induced phase transitions in alkali halide crystals", *Phys. Rev.*, **B12**, 3228 (1975).
[88] C.W. Muhlhausen and R.G. Gordon, "Density-functional theory for the energy of crystals: Test of the ionic model", *Phys. Rev.*, **B24**, 2147 (1981).
[89] J. Kendrick and W.C. Mackrodt, "Interatomic potentials for ionic materials from first principles calculations", *Solid State Ionics*, **8**, 247 (1983).
[90] J.H. Harding and A.H. Harker, "Calculations of Inter-ionic Potentials in Oxides", *Phil. Mag.*, **B51**, 119 (1985).
[91] R.P. McEachran, A.D. Stauffer and S. Greita, "Polarizabilities and shielding factors for the noble gas isoelectronic sequences", *J. Phys. B*, **12**, 3119 (1979).